Gravitational footprints of massive neutrinos and lepton number breaking

Antonino Marcianò

Fudan University

A.Addazi, A. Marciano, A. Morais, R. Pasechnik, R. Sistrava & Jose W.F. Valle
arXiv:1909.09740 (PLB 2020)

P. Dona, A. Marciano, Y. Zhang & C. Antolini, arXiv:1509.05824 (PRD 2016)

A.Addazi, A. Marciano & R. Pasechnik, arXiv:1812.07376 (CPC 2019)

A.Addazi, A. Marciano & R. Pasechnik, arXiv:1804.09826 (EPJC 2019)

work in progress…

XXIII Bled (Virtual) Workshop, VIA platform, 6-10 July 2020

Plan of the talk

The multi-messenger approach & particle physics

GW & tests of DM models from binary systems EoS

GW generated by FOPT

Neutrino physics and the mass-generation

See-saw mechanism and GW production

Partial conclusions

The multi-messenger approach & particle physics

The multi-messenger approach

Electro-magnetism
Neutrinos
Comic rays
GW signals

Use gravitational waves to probe high and low-scale physics

Ex. : LISA, U-DECIGO and BBO can test SSB in 10 GeV-10 TeV

Ex. : PTA, SKA, FAST (nHz range) can test in MeV-ish scales

Cross-checking strategy: meson factories, LHC, CEPC, etc…

Recurrent questions

What is the nature of Dark Matter?

Can we use Gravitational Waves to unveil its nature?

Can we use a cross-checking multi messenger strategy?
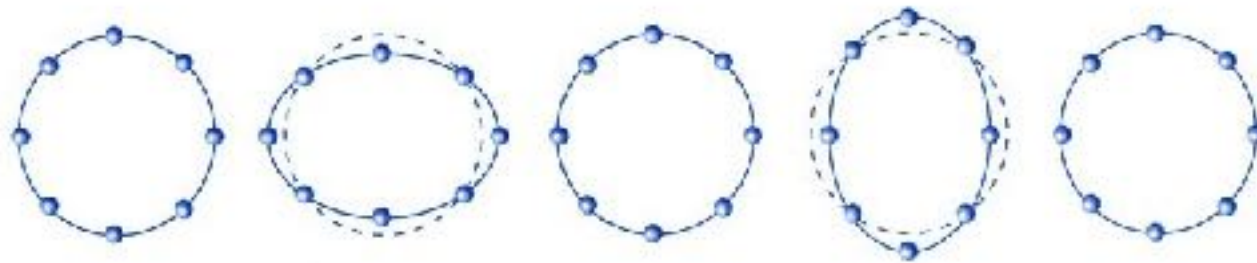
How does neutrinos' mass generate?

Can we understand the nature of the inflaton?

What can we infer about confinement in QCD?

We deploy at the same time informations from different observational channels!
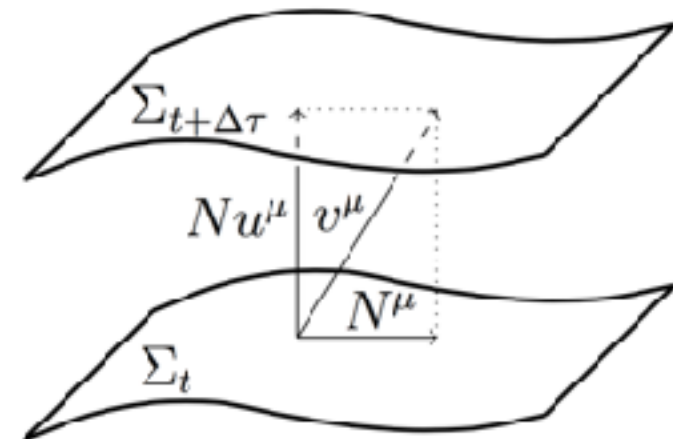
Gravitational Waves

$$g_{\mu\nu} = \eta_{\mu\nu} + h_{\mu\nu}$$

2 propagating d.o.f.

$$\frac{1}{c^2}\frac{\partial^2}{\partial t^2} - \nabla^2 h_{ij}(\mathbf{x}, t) = \frac{16\pi G}{c^4} S_{ij}(\mathbf{x}, t)$$
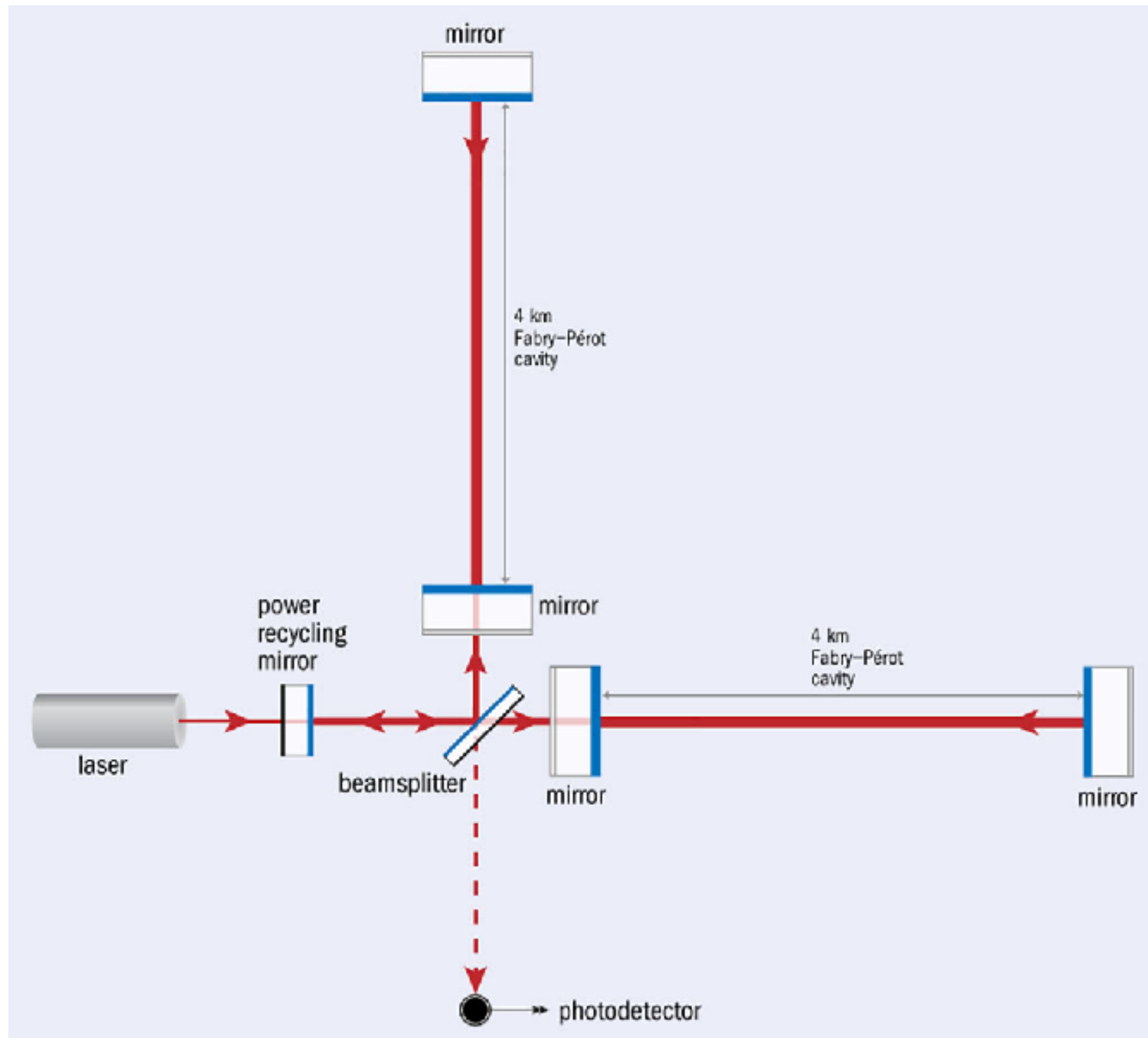
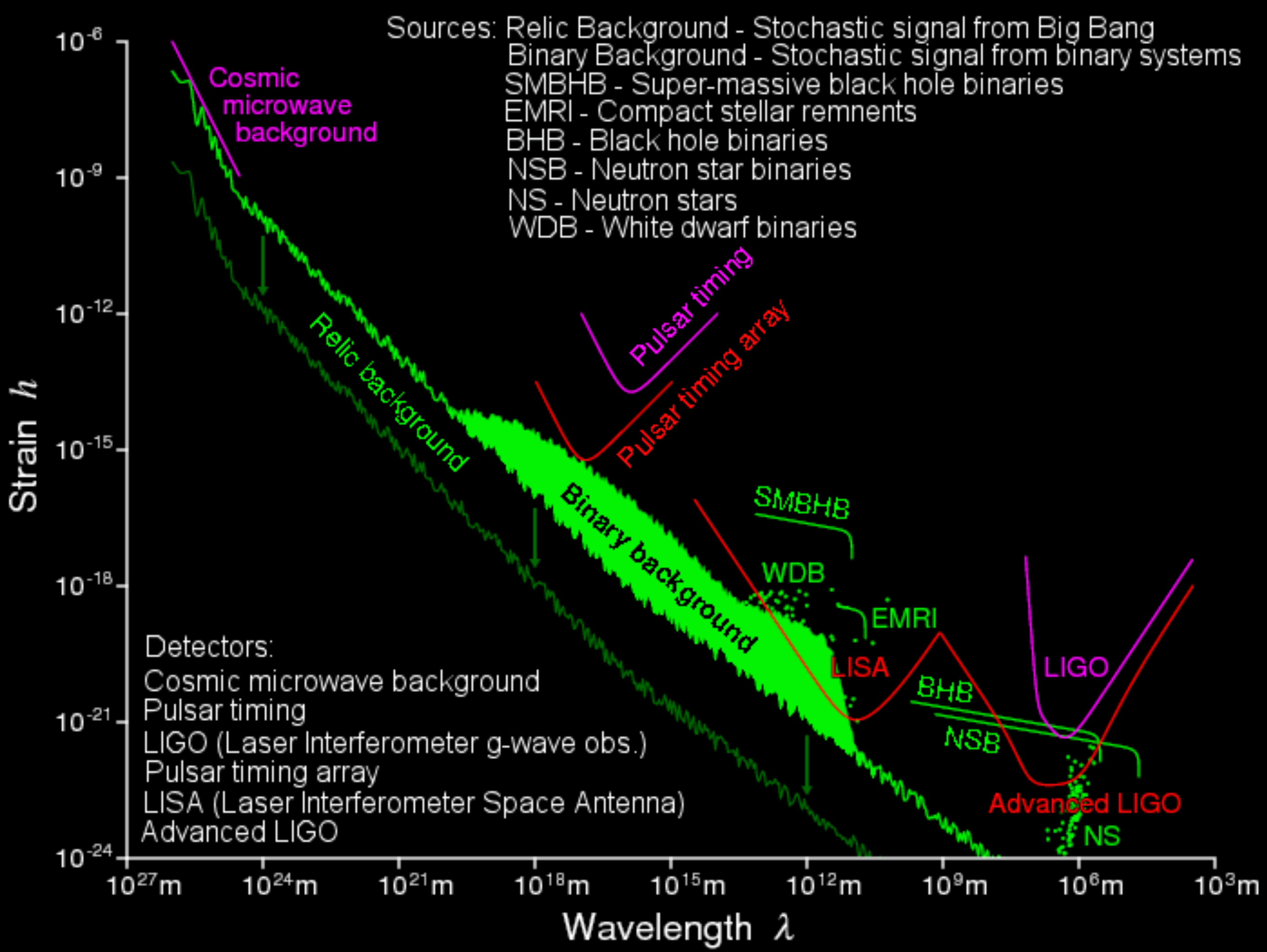$$S_{ij}(\mathbf{x}, t) \equiv T_{ij}(\mathbf{x}, t) - \frac{1}{3}\delta_{ij}T^k{}_k(\mathbf{x}, t)$$
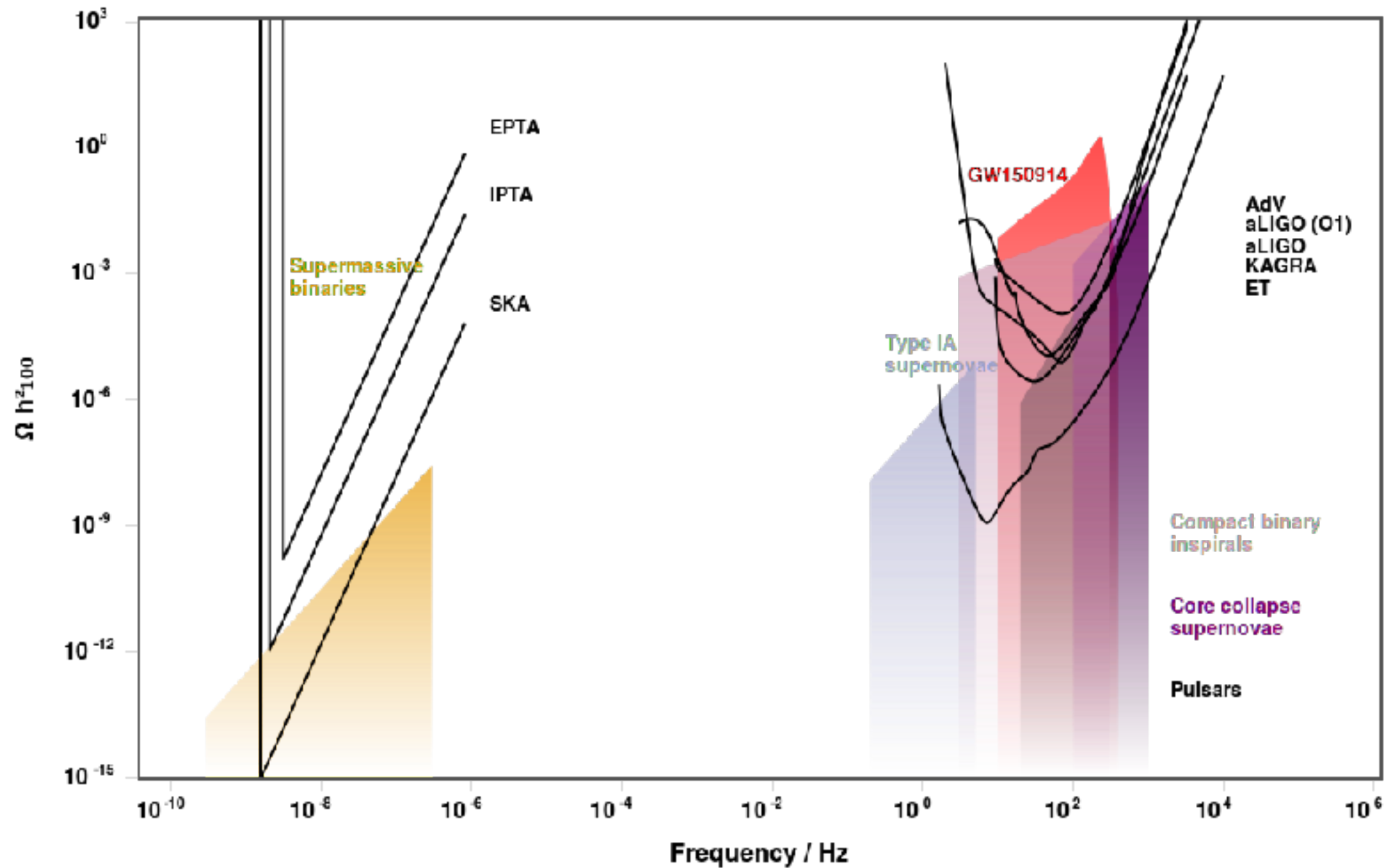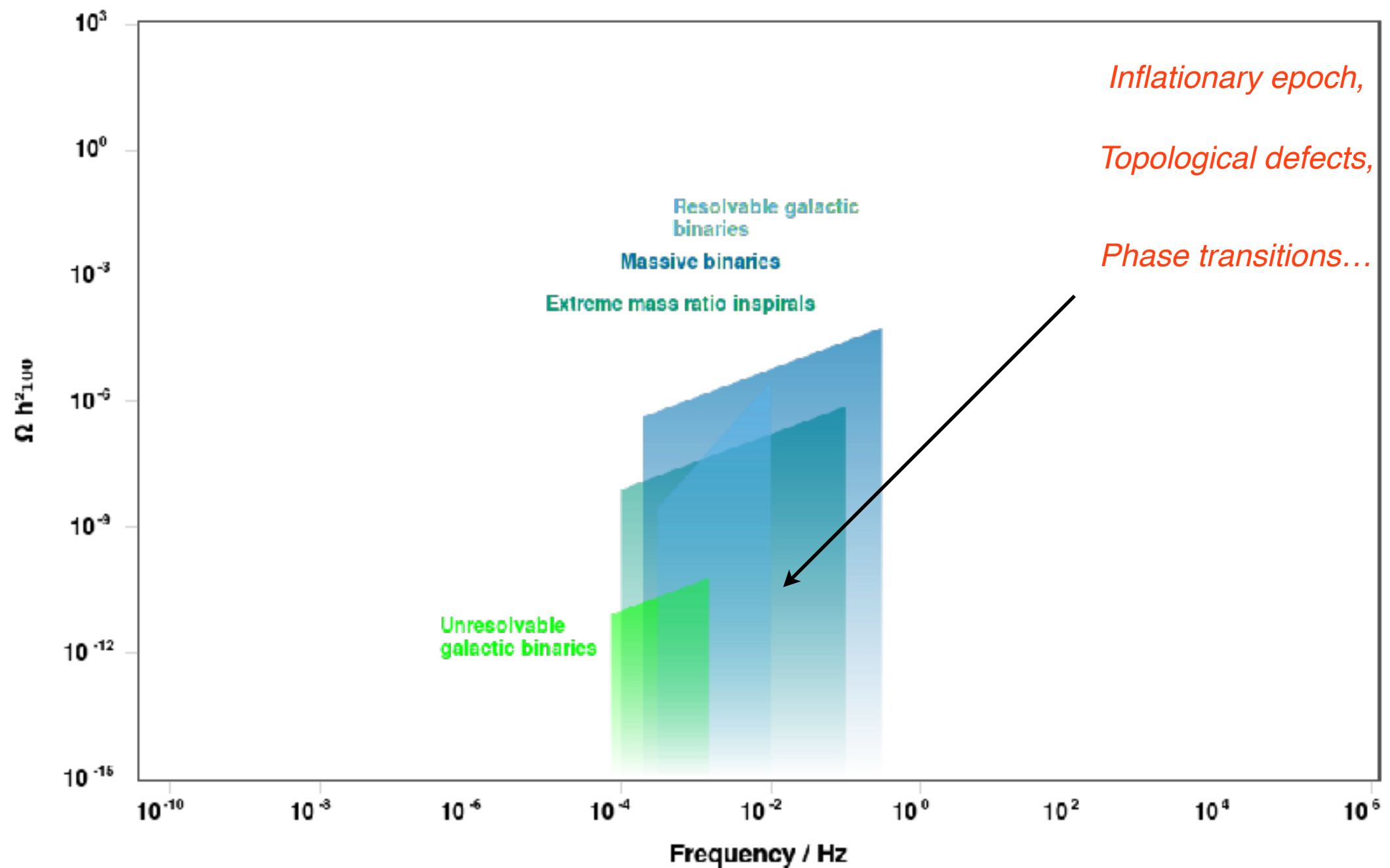
Gravitational Waves

Gravitational Waves

Sources: Relic Background - Stochastic signal from Big Bang
Binary Background - Stochastic signal from binary systems
SMBHB - Super-massive black hole binaries
EMRI - Compact stellar remnents
BHB - Black hole binaries
NSB - Neutron star binaries
NS - Neutron stars
WDB - White dwarf binaries

Detectors:
Cosmic microwave background
Pulsar timing
LIGO (Laser Interferometer g-wave obs.)
Pulsar timing array
LISA (Laser Interferometer Space Antenna)
Advanced LIGO

Gravitational Waves

Credit: G. Nardini (Lisa collaboration), Fudan 2017

XXIII Bled (Virtual) Workshop, VIA platform, 6-10 July 2020

Gravitational Waves

Credit: G. Nardini (Lisa collaboration), Fudan 2017

XXIII Bled (Virtual) Workshop, VIA platform, 6-10 July 2020

First observations of Gravitational Waves

Inspiral   Merger   Ringdown

Tidal forces and celestial objects

The response of each star to external disturbance is described by the Love numbers

Radius of the star

$$Q_{ij} = -k_2 \frac{2R^5}{3G} E_{ij} \equiv -\lambda E_{ij}$$

Applied tidal field

Induced quadrupole moment
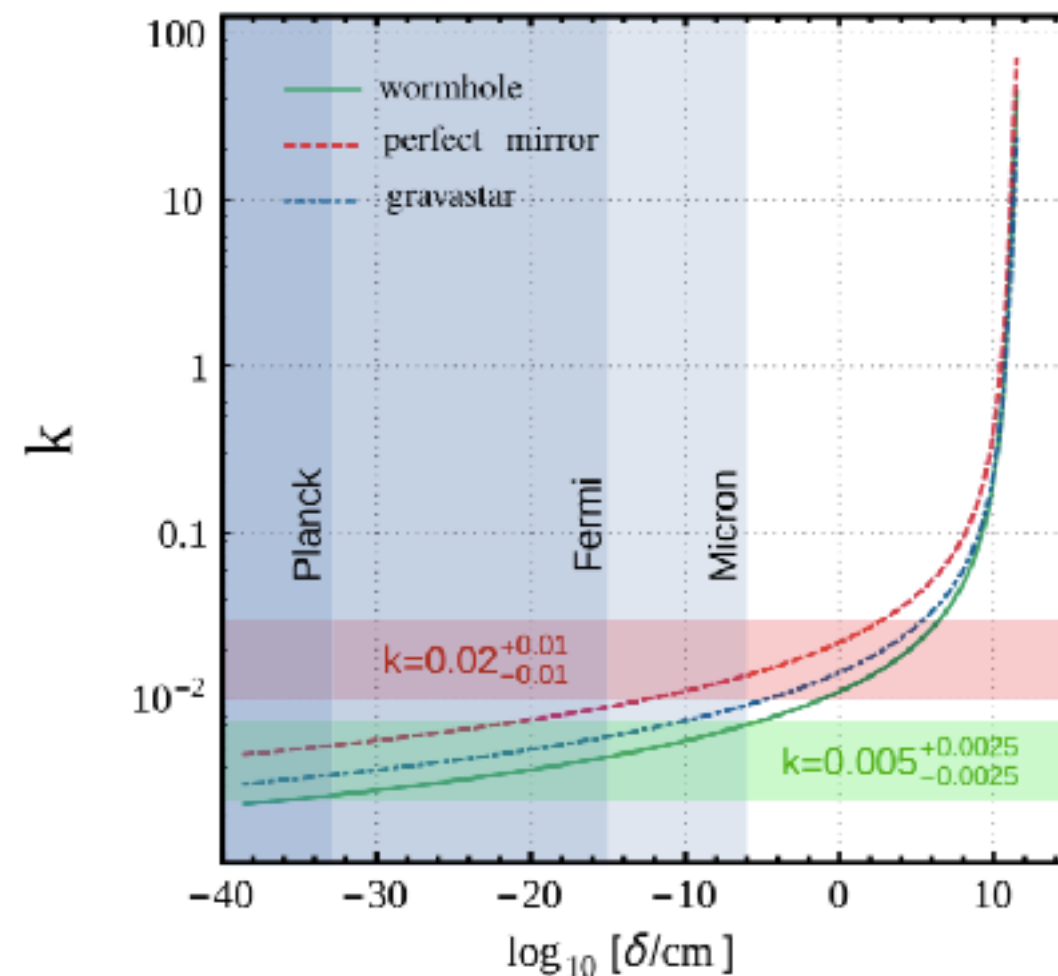
ECOs and their Love numbers

From the Love number of an ECO, can one infer additional near horizon physics?

Maselli et al. , PRL 120, 081101 (2018)

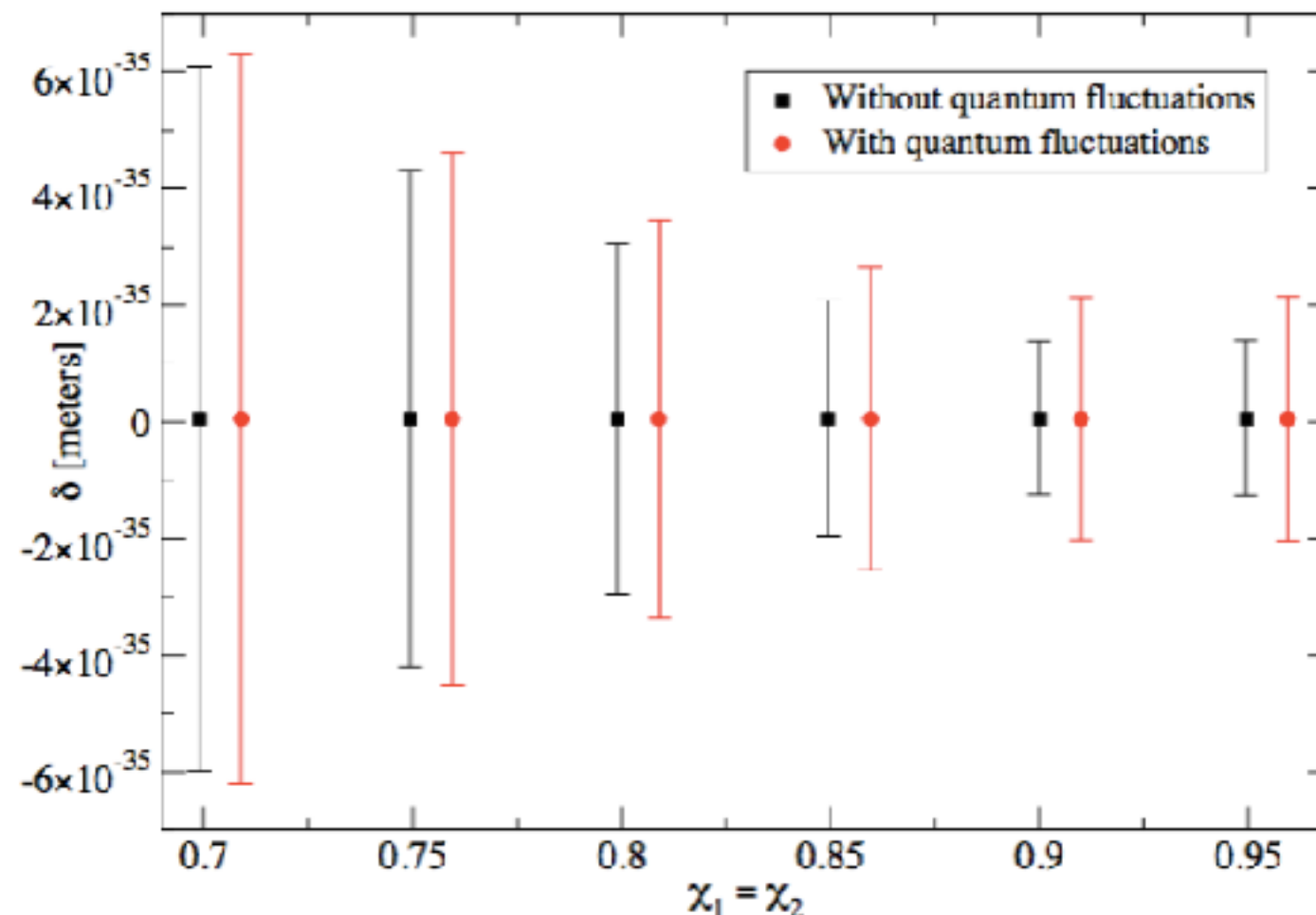$$\delta = r_0 - r_H = r_H e^{-1/k}$$

Encoding quantum fuzziness

Quantum fluctuations in the signal blur or fuzz out its amplitude and phase

$$\frac{\sigma_\delta^{\text{tot}}}{\hat{\delta}} = \sqrt{\left(\frac{\sigma_M^{\text{stat}}}{\hat{M}}\right)^2 + \frac{1}{\hat{k}^2}\left(\frac{\sigma_k^{\text{stat}}}{\hat{k}}\right)^2 + \frac{a^2 \ell_{\text{Pl}}^2}{\hat{\delta}^2}}$$
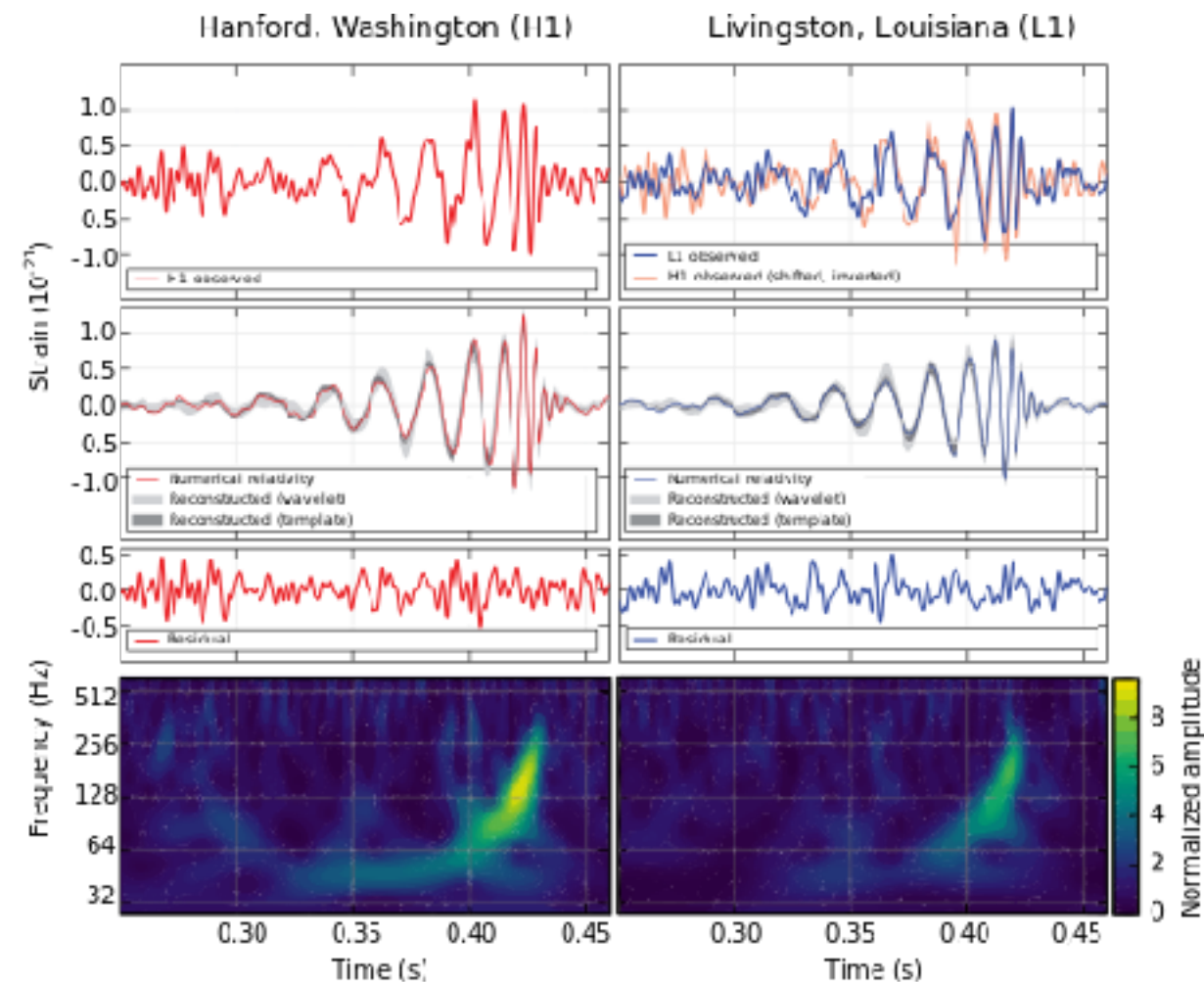
First observations of Gravitational Waves

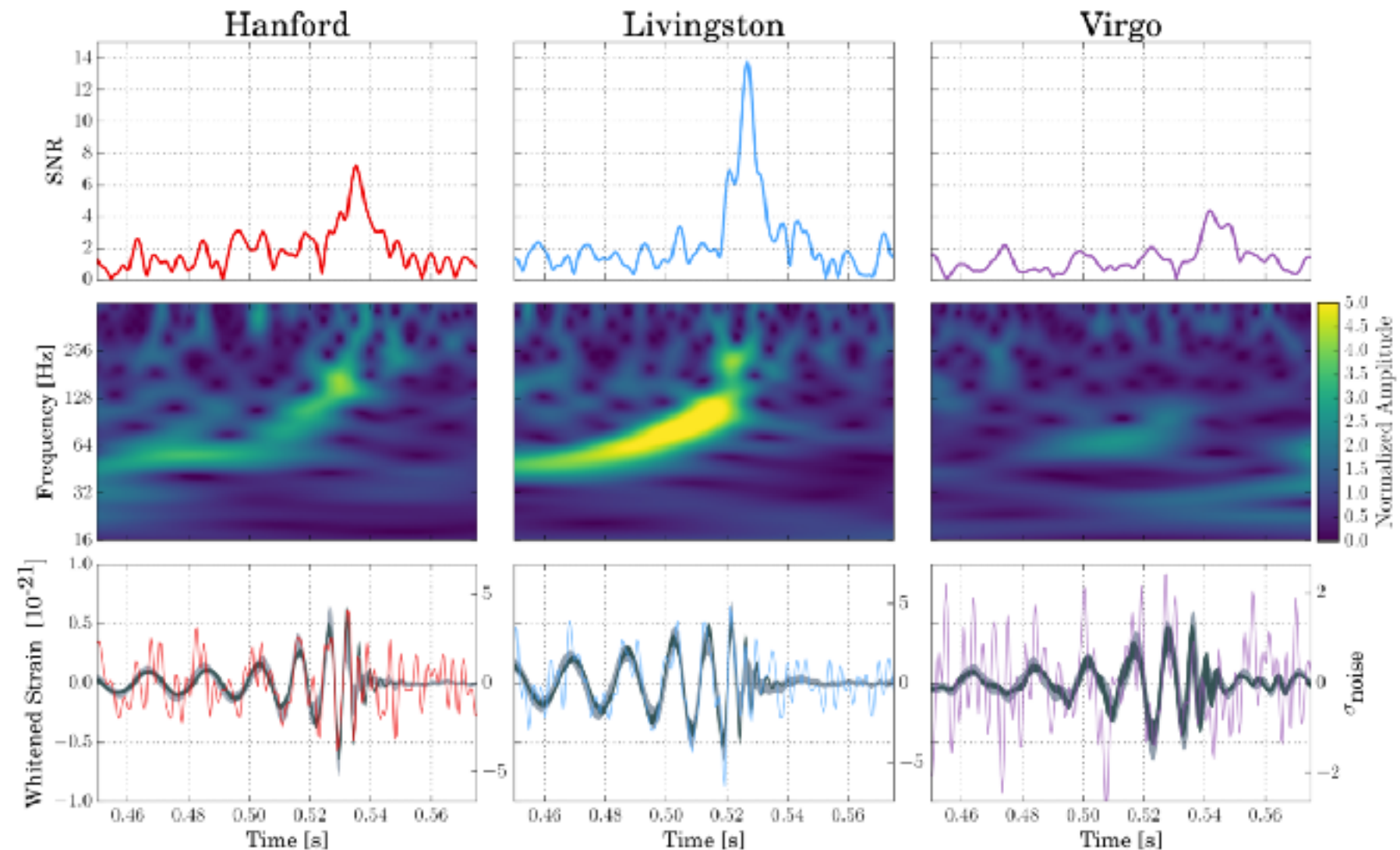## GW150914

Distance ~ 440 Mpc

~3 solar masses emitted in GW
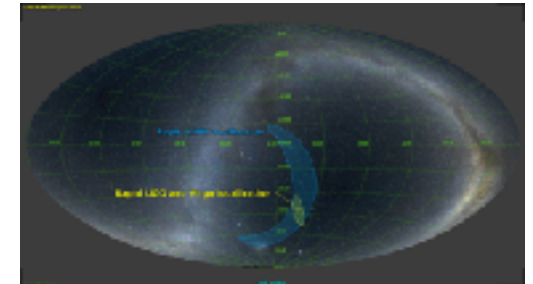
First observations of Gravitational Waves

GW170814

Distance ~ 540 Mpc

~3 solar masses emitted in GW

Multi-messenger perspective for Dark Matter

GW170817
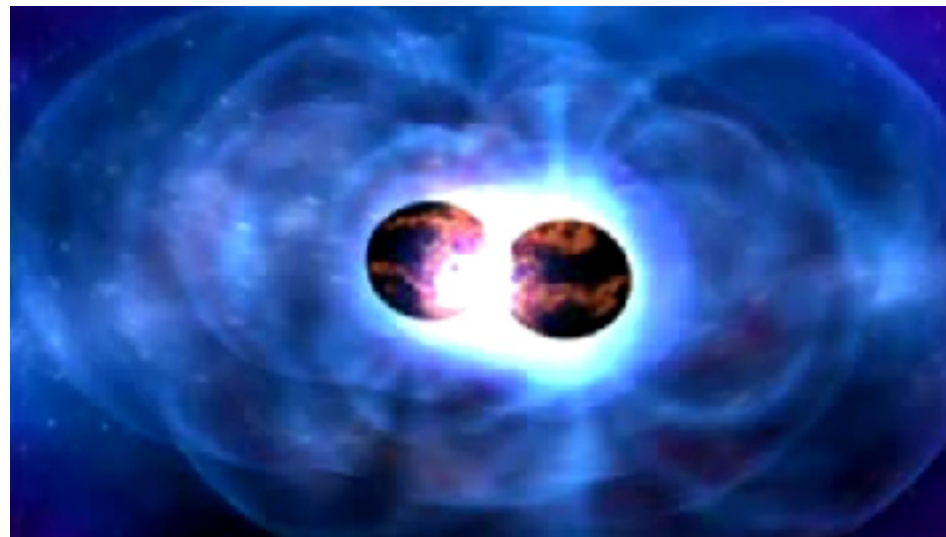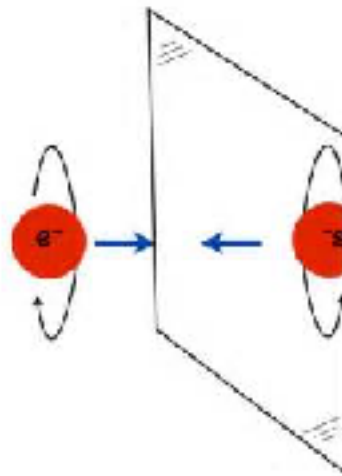
GRB170817A

Distance ~ 40 Mpc

Neutron stars around 1 and 2 solar masses

Multi-messenger perspective for Dark Matter

A. Addazi & A. Marciano, IJMPA 2018; A. Addazi, R. Ciancarella, F. Pannarale, A. Marciano (in preparation)

XXIII Bled (Virtual) Workshop, VIA platform, 6-10 July 2020
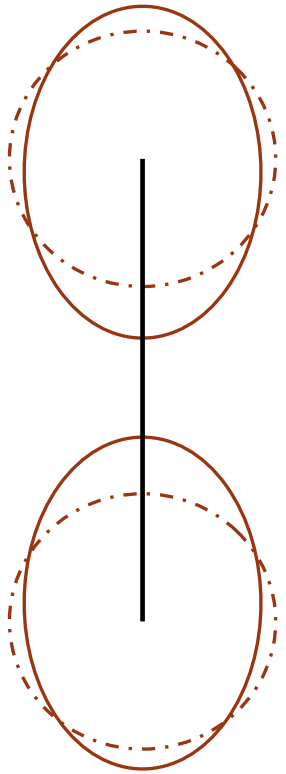
Equations of State for Neutron Stars

$$Q_{ij} = -\lambda \varepsilon_{ij}$$

*Solve static equilibrium equations (TOV)
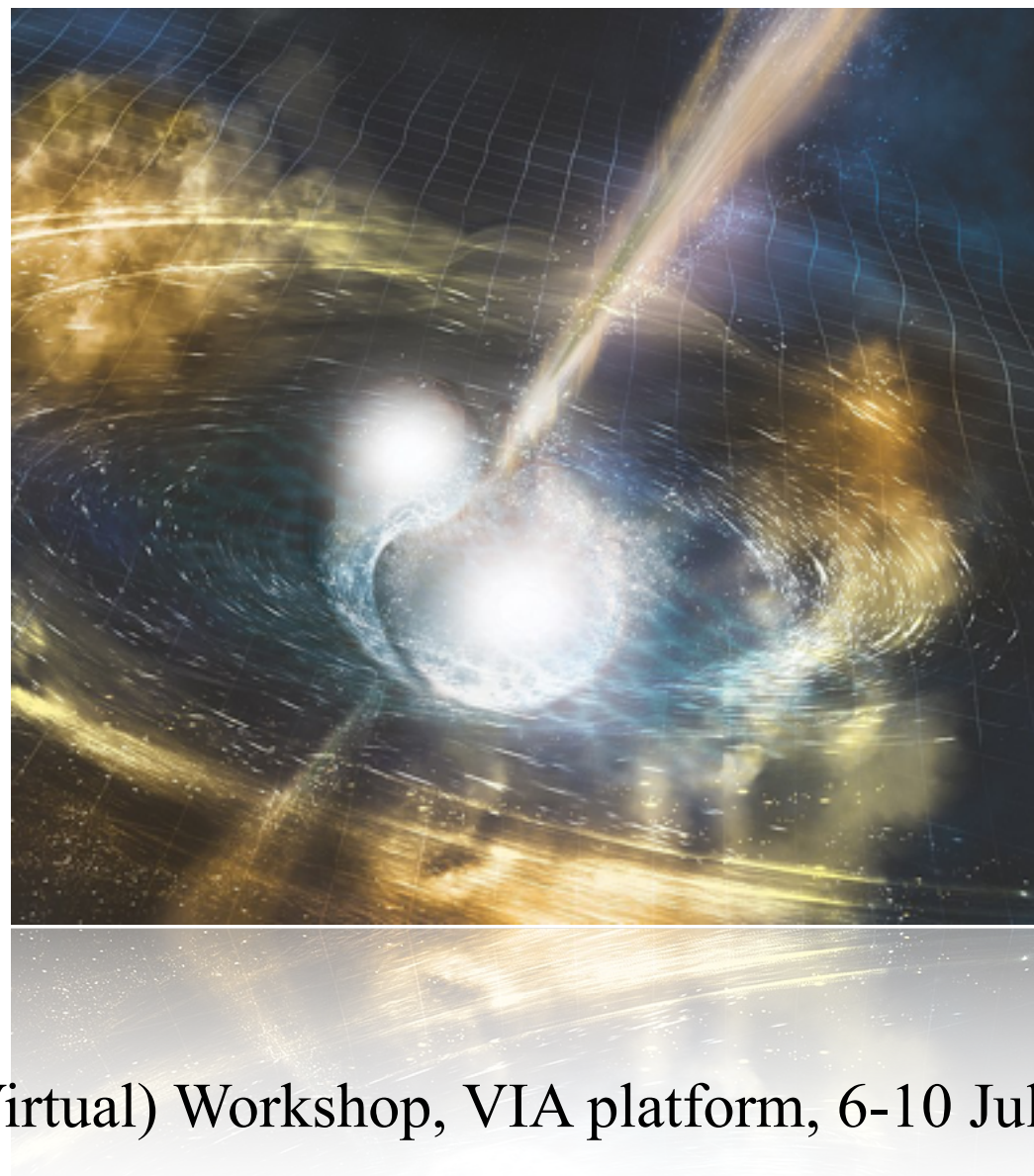and second order differential equations Hinderer (2010)*

$$\Lambda = \frac{\lambda}{M^5}$$

$$\Lambda_{GW170817} = 190^{+390}_{-120}$$

Measuring NS deformability $\longrightarrow$ matter in density regimes inaccessible on Earth

Pions presence, nontrivial fluidodynamics… $\longrightarrow$

Anisotropic models
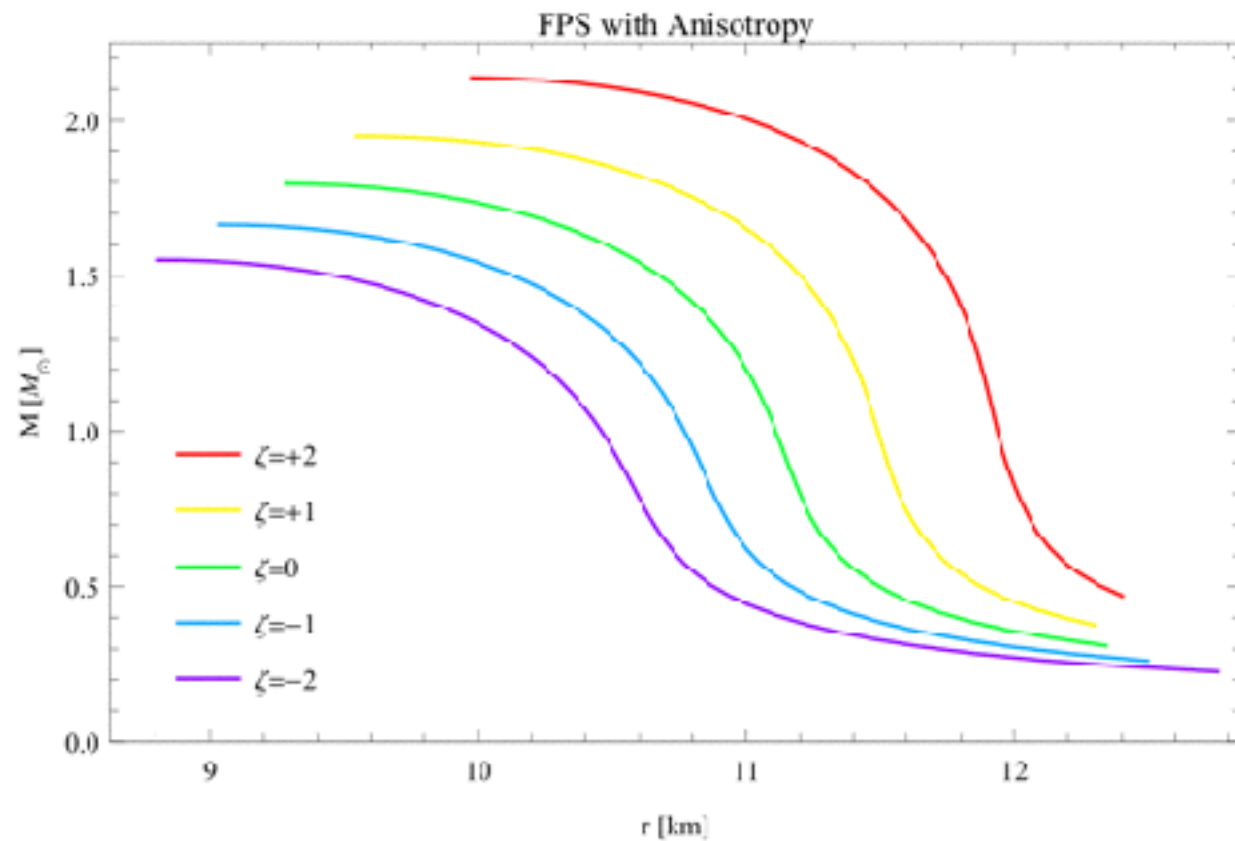
$$p_t(r) = p_r + \frac{\zeta}{3}\frac{r(\varepsilon - 3p_r)}{r - 2m(r)}(\varepsilon - p_r)r^2$$

Bowers & Liang 1974
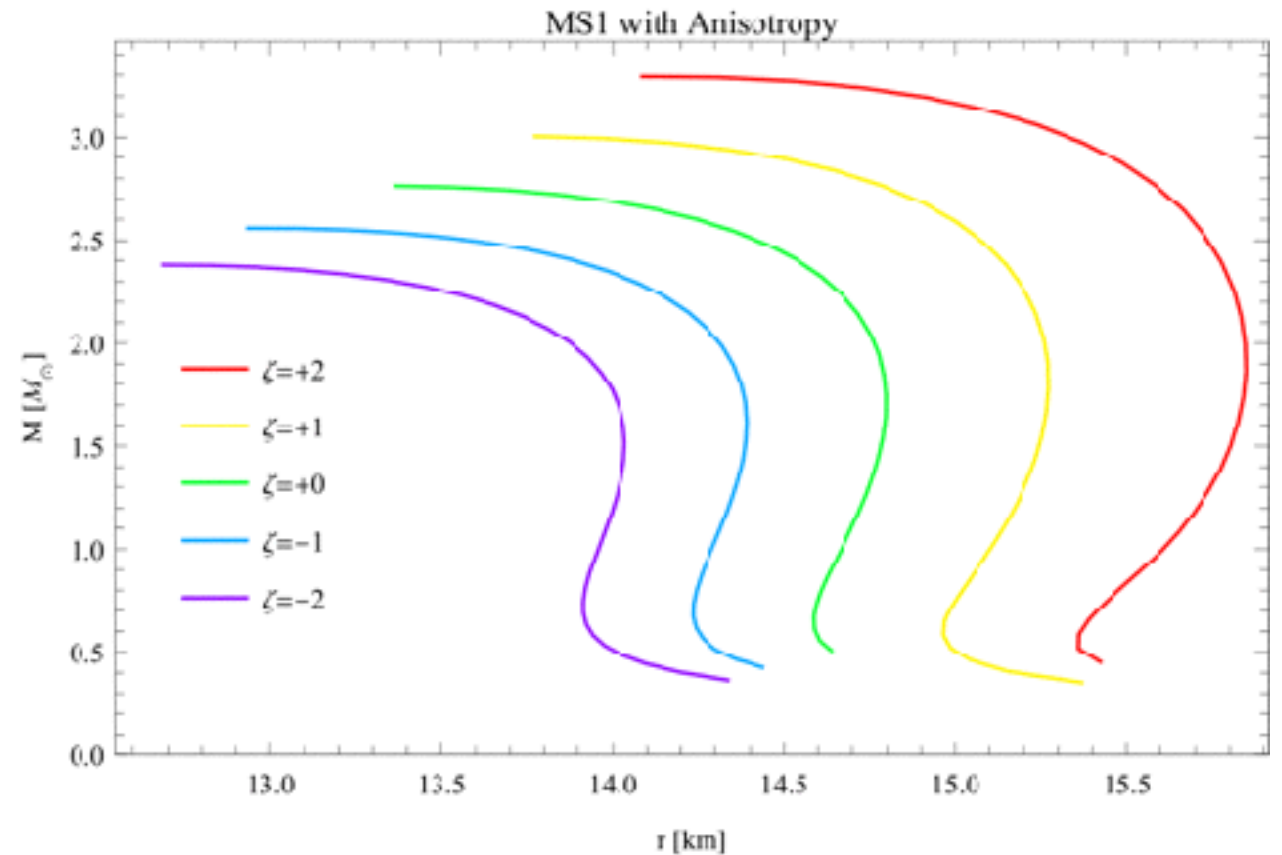
Role of anisotropies in NS EoS I

A. Addazi, R. Ciancarella, A. Marciano & F. Pannarale
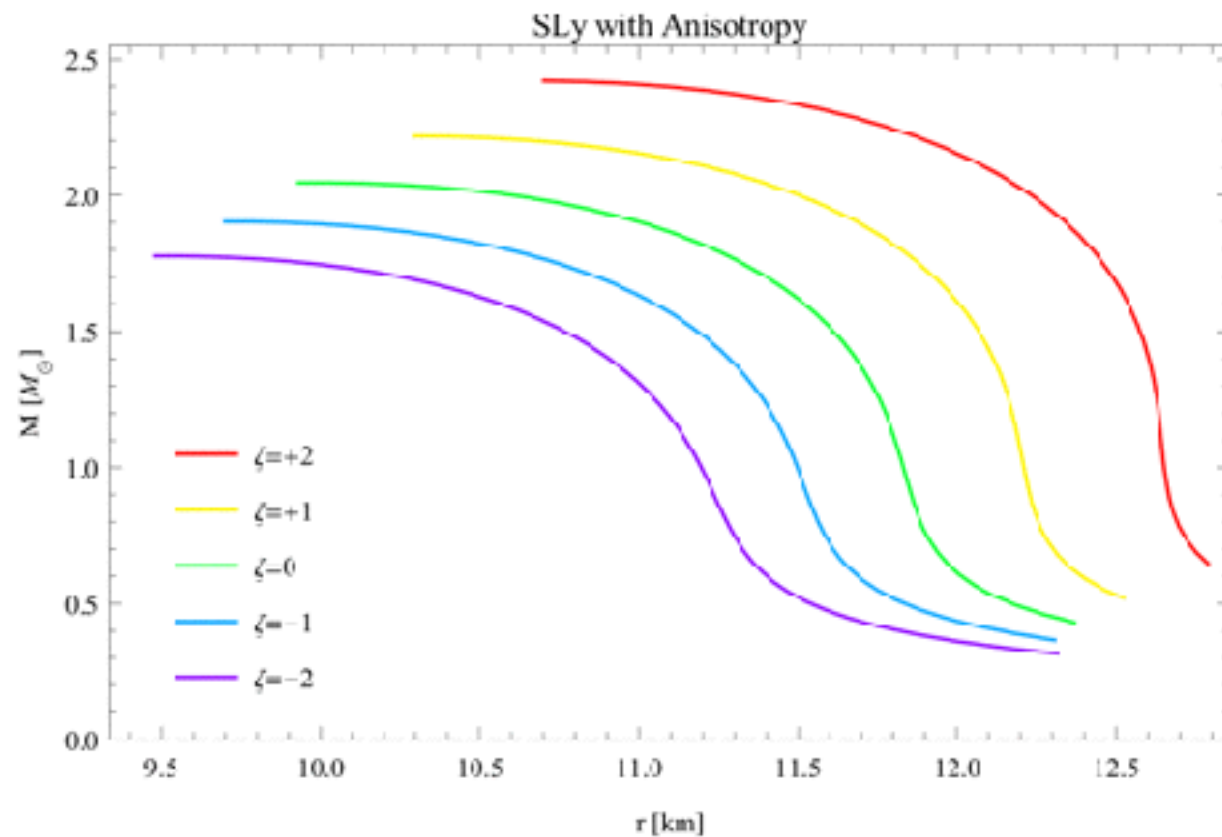
Role of anisotropies in NS EoS II

SLy with Anisotropy

	$\zeta = +2$	$\zeta = +1$	$\zeta = -1$	$\zeta = -2$
R(km)	12.60	12.11	11.28	10.91
C	0.164	0.171	0.183	0.190
k_2	0.0952	0.0829	0.0663	0.0608
$\lambda(10^{36}\,\mathrm{g\,cm^2\,s^2})$	3.02	2.16	1.21	0.93

$\zeta > 0$

Maximal mass at fixed central pressure increases.
Tidal deformability increases while compactness decreases.

$\zeta < 0$
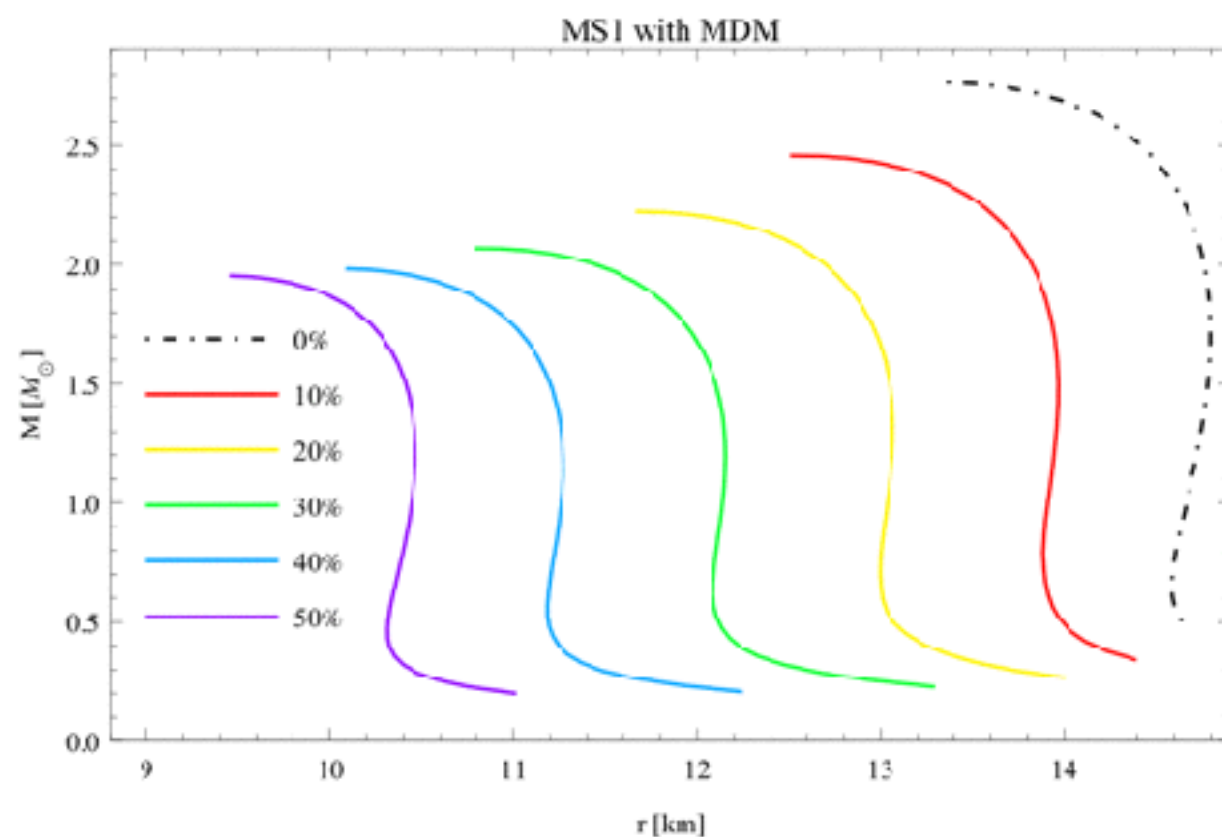
Maximal mass at fixed central pressure decreases.
Tidal deformability decreases while compactness increases.

Mirror Dark Matter I

Following T.D. Lee & C. Yang (1956), parity, as a global symmetry, might be restored in a dark sector:

- *The Dark Sector as copy of the Standard Model, with opposite chirality*

- *Different nucleosynthesis*

- *Interacting either gravitationally or weakly coupled to EM*

MS1 with MDM

0%<MDM<50%

Maximal mass decreases at fixed central pressure.
Tidal deformability decreases while compactness increases.
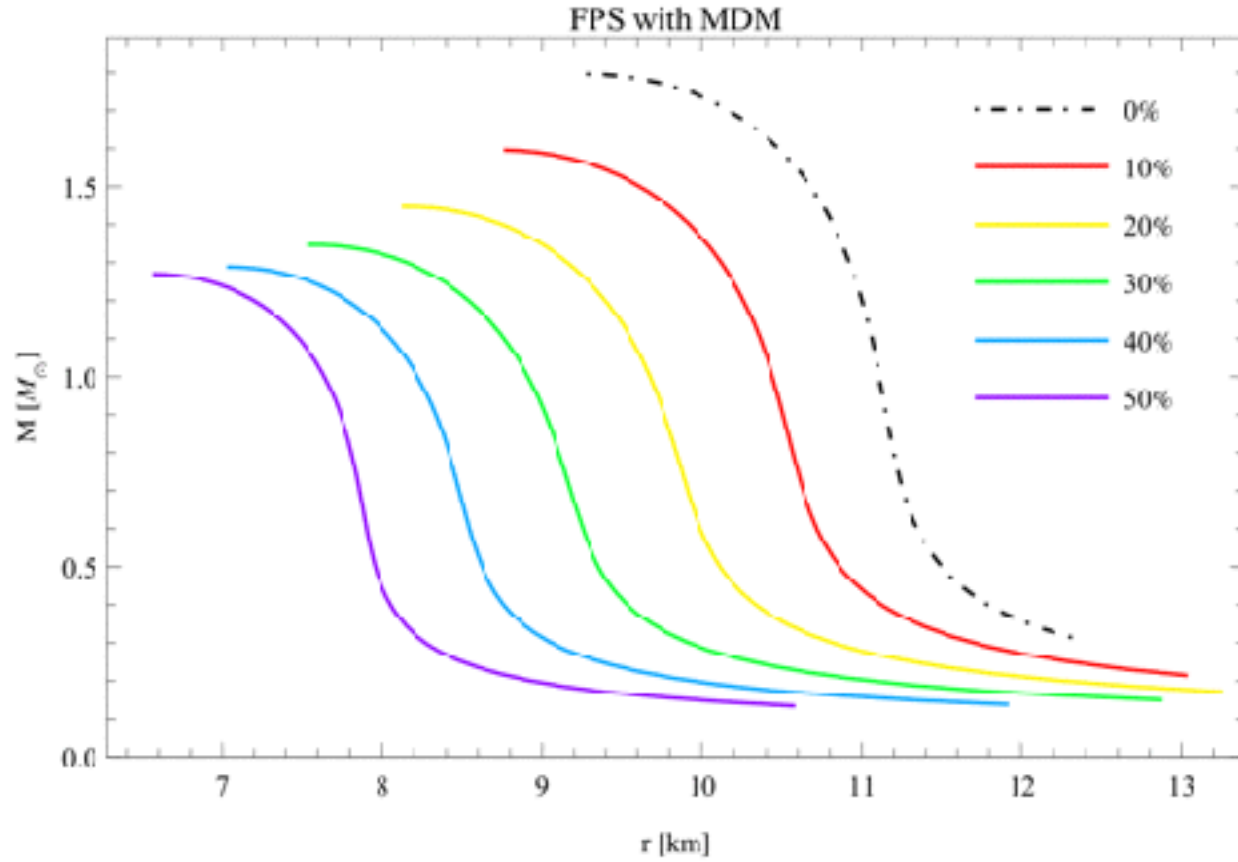
MDM>50%
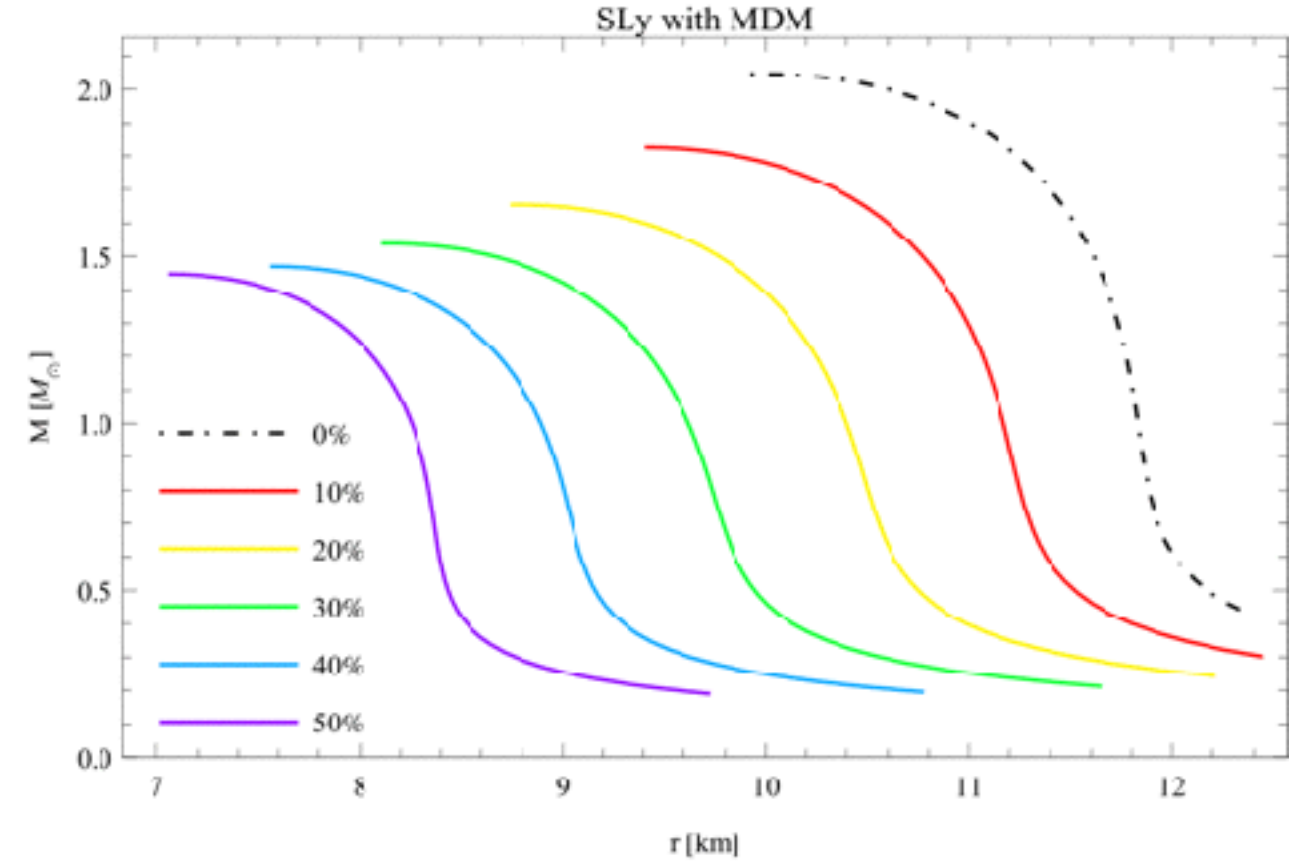
Specular to the case above

MS1 with MDM					
	10%	**20%**	**30%**	**40%**	**50%**
R(km)	13.97	13.06	12.13	11.24	10.44
C	0.148	0.158	0.170	0.184	0.198
k_2	0.0838	0.0737	0.0647	0.0623	0.0676
$\lambda(10^{36}\,\mathrm{g\,cm^2\,s^2})$	4.44	2.80	1.70	1.12	0.839

Mirror Dark Matter II

FPS with MDM

	10%	**20%**	**30%**	**40%**	**50%**
R (km)	10.36	9.56	8.76	8.06	7.47
C	0.157	0.170	0.185	0.202	0.217
k_2	0.0724	0.0605	0.0535	0.0508	0.0523
$\lambda (10^{36}\,\mathrm{g\,cm^2\,s^2})$	0.865	0.482	0.276	0.172	0.124
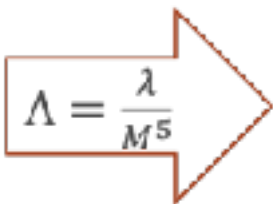
SLy with MDM

	10%	**20%**	**30%**	**40%**	**50%**
R(km)	10.90	9.98	9.06	8.22	7.57
C	0.190	0.207	0.228	0.251	0.273
k_2	0.0600	0.0485	0.0404	0.0352	0.0333
$\lambda (10^{36}\,\mathrm{g\,cm^2\,s^2})$	0.921	0.481	0.247	0.132	0.0831

Confronting with GW170817 and PSR J0349+4032

Inferred Mass from PSR
J0348+4032

$$M = (1.97 \div 2.05) M_\odot$$

% of MDM	0%	10%	20%	30%	40%	50%
SLy	**282**	163	85	44	23	15
MS1	1246	786	**495**	**301**	**197**	148

Tidal deformability from GW170817

$$\Lambda_{GW170817} = 190^{+390}_{-120}$$

$$\Lambda = \frac{\lambda}{M^5}$$

ζ	+2	+1	0	-1	-2
FPS	**349**	240	172	121	84
SLy	**534**	**381**	**282**	214	165
MS1	2242	1645	1246	979	807

Necessary condition

Given either the families EoS-ζ or EoS-MDM, there must be a sequence that satisfies PSR J0348+4032 and a sequence that satisfies GW170817

Within the range assumed:
a) MS1 is rejected for the anisotropic case
b) FPS is rejected in the MDM case
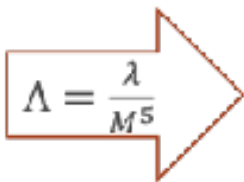
Confronting with GW170817 and PSR J0349+4032

Inferred Mass from PSR
J0348+4032

$$M = (1.97 \div 2.05) M_\odot$$

% of MDM	0%	10%	20%	30%	40%	50%
SLy	**282**	163	85	44	23	15
MS1	1246	786	**495**	**301**	**197**	148

Tidal deformability from GW170817

$$\Lambda_{GW170817} = 190^{+390}_{-120}$$

$\Lambda = \dfrac{\lambda}{M^5}$

ζ	+2	+1	0	-1	-2
FPS	**349**	240	172	121	84
SLy	**534**	**381**	**282**	214	165
MS1	2242	1645	1246	979	807

Sufficient condition

Given either the families EoS-ζ or EoS-MDM, there must be at least a
sequence satisfying at the same time PSR J0348+4032 e GW170817

Future perspective on NS EoS and (M)DM

Anisotropies

Several configurations EoS-ζ satisfy constraints separately. Other satisfy both the constraints

MS1 is rejected in the anisotropic case

FPS must be reconsidered, since it turns out that it can still be valid

Mirror Dark Matter

FPS is rejected in presence of MDM.

MS1 must be reconsidered, since it turns out that can be still valid.

Recover tidal deformability for different EoS

Implement different model of dark matter

Develop template for wave-forms

Confrontation with the EM channel!

GW generated by FOPT
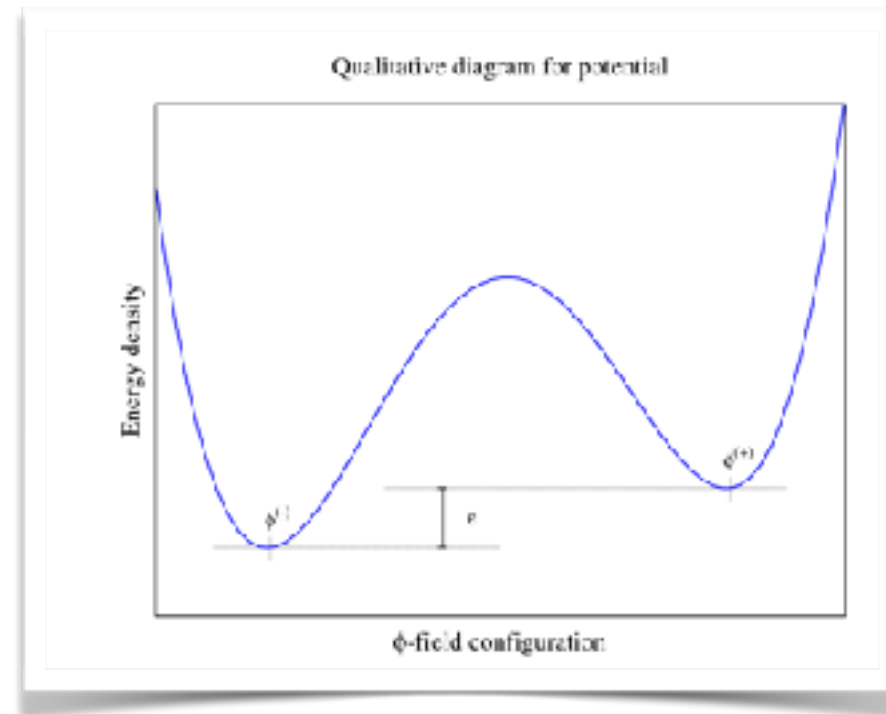
Gravitational Waves Stochastic Background

Signal from unresolved astrophysical sources
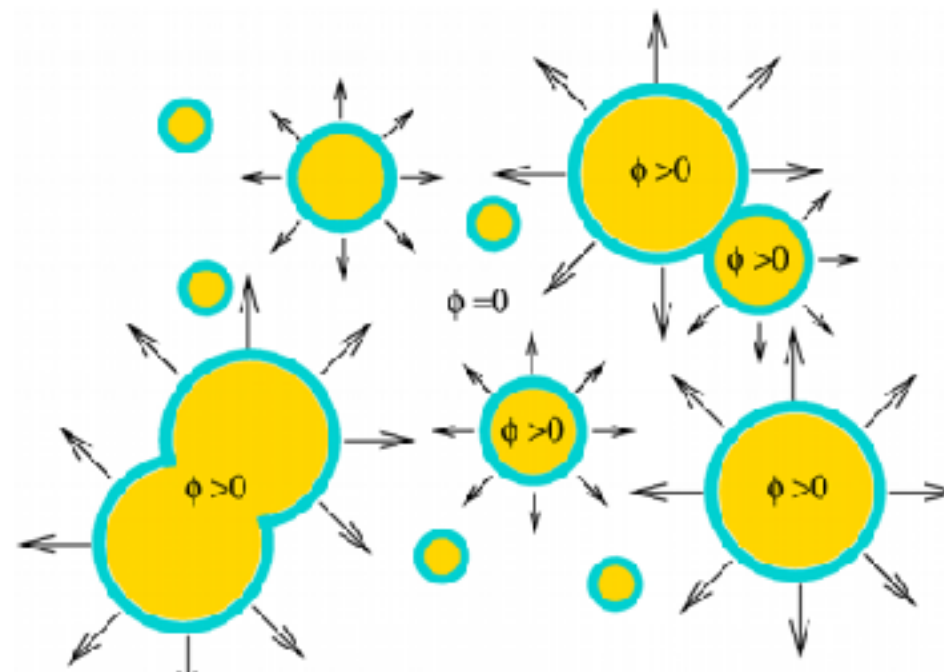
Signal from cosmological events

i) Early cosmology (inflation, bouncing cosmologies, string gas cosmology etc…)

ii) Cosmic strings

iii) Strong Cosmological Phase Transitions

Tunnelling and bubbles enucleation

Coleman, Frampton etc…

Latent energy parameter

Normalized difference between minima

$$\mathcal{E}(\bar{T}) = \left[T \frac{dV_{eff}}{dT} - V_{eff}(T) \right]_{T=\bar{T}}$$

$$\alpha = \frac{\mathcal{E}(\bar{T})}{\rho_{rad}(\bar{T})} \qquad \rho_{rad} = \frac{\pi^2}{30} g_*(T) T^4$$

Latent Energy

Bubble nucleation parameter

How fast the minimum goes down

$$\beta = -\left[\frac{dS_E}{dt}\right]_{t=\bar{t}} \simeq \left[\frac{1}{\Gamma}\frac{d\Gamma}{dt}\right]_{t=\bar{t}},$$

$$S_E(T) \simeq \frac{S_3(T)}{T} \qquad \Gamma = \Gamma_0(T)\exp[-S_E(T)]$$

$$\Gamma_0(T) \sim T^4, \;\; S_3 \equiv \int d^3r\left(\partial_i s^\dagger \partial_i s + V_{eff}(s,T)\right)$$

β/*H* *provides an inverse time scale*

Effective action

Relation between size of the bubble wall and bubble velocity

$$d \simeq \frac{V_B}{\beta}$$

Effective potential

$$V_{tree}(s, T = 0) + V_1(s, T)$$

$$V_1(s, T) = V_{CW}(s, T = 0) + \Delta V(s, T)$$

Bubbles collision

$$\nu_{collision} \simeq 3.5 \times 10^{-4} \left(\frac{\beta}{H_*} \right) \left(\frac{\bar{T}}{10\,\mathrm{GeV}} \right) \left(\frac{g_*(\bar{T})}{10} \right)^{1/6} \mathrm{mHz}$$

frequency is proportional to temperature

$$\Omega_{collision}(\nu_{collision}) \simeq C\mathcal{E}^2 \left(\frac{\bar{H}}{\beta} \right)^2 \left(\frac{\alpha}{1+\alpha} \right)^2 \left(\frac{V_B^3}{0.24 + V_B^3} \right) \left(\frac{10}{g_*(\bar{T})} \right)$$

$$C \simeq 2.4 \times 10^{-6}$$

corresponding intensity

$h^2 \Omega_{\mathrm{col}}$ dominates for large wall velocities $v_b \to 1$

$$h^2 \Omega \left(f; \alpha, \beta/H, f_{\mathrm{peak}} \right) \qquad f_{\mathrm{peak}} \left(\alpha, \beta/H, T_n \right)$$

Shock waves and turbulence

$$f_{\mathrm{SW}}[\mathrm{Hz}] = 1.9 \times 10^{-5} \frac{\beta}{H} \frac{1}{v_b} \left(\frac{T_n}{100\,\mathrm{GeV}} \right) \left(\frac{g_*}{100} \right)^{1/6}$$

$$f_{\mathrm{MHD}}[\mathrm{Hz}] = 2.7 \times 10^{-5} \frac{\beta}{H} \frac{1}{v_b} \left(\frac{T_n}{100\,\mathrm{GeV}} \right) \left(\frac{g_*}{100} \right)^{1/6}$$

frequency is proportional to temperature

$$h^2 \Omega_{\mathrm{SW}}(f) = 2.65 \times 10^{-6} \left(\frac{\beta}{H} \right)^{-1} \left(\frac{\kappa_v \alpha}{1+\alpha} \right)^2 \left(\frac{g_*}{100} \right)^{-1/3} v_b \left(\frac{f}{f_{\mathrm{SW}}} \right)^3 \left(\frac{7}{4+3(f/f_{\mathrm{SW}})^2} \right)^{7/2}$$

$$h^2 \Omega_{\mathrm{MHD}}(f) = 3.35 \times 10^{-4} \left(\frac{\beta}{H} \right)^{-1} \left(\frac{\kappa_{\mathrm{turb}} \alpha}{1+\alpha} \right)^{3/2} \left(\frac{g_*}{100} \right)^{-1/3} v_b \left(\frac{f}{f_{\mathrm{MHD}}} \right)^3 \left(\frac{(1+f/f_{\mathrm{MHD}})^{-11/3}}{1+8\pi f/h_*} \right)$$

corresponding intensity

Velocity enhancement
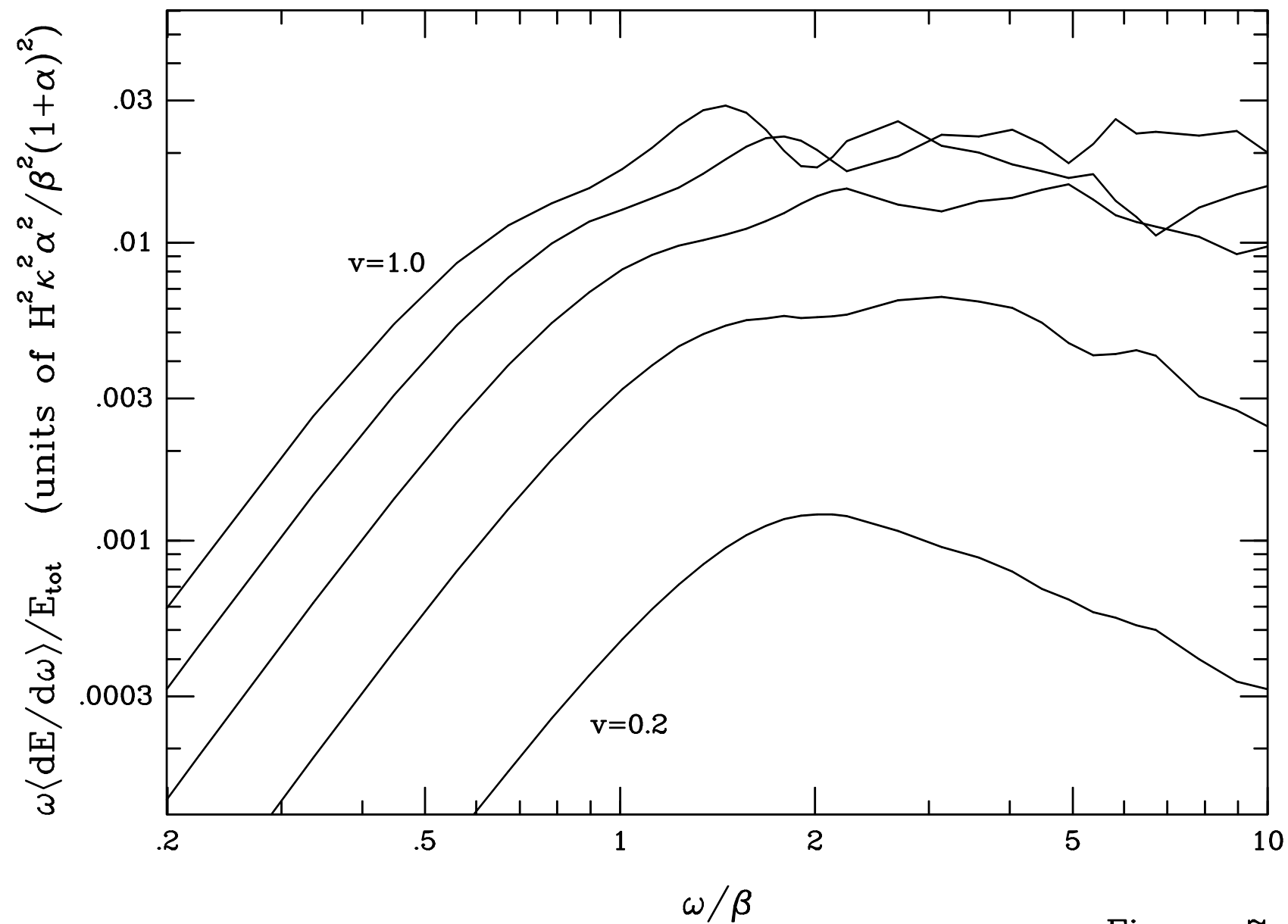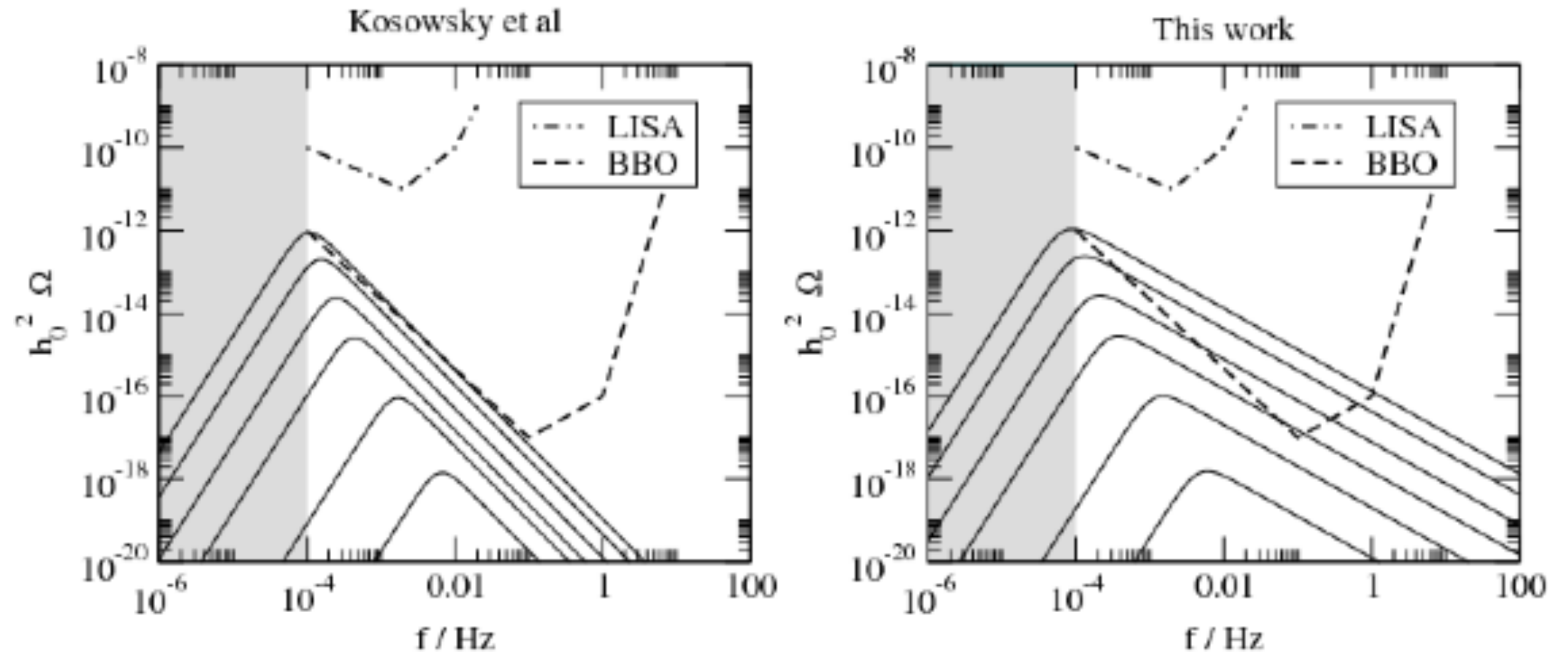
Figure 7

Kamionkowski, Kosowsky, Turner 1994

Credit: A. Kosowsky, Fudan Spring School of Cosmology 2017

XXIII Bled (Virtual) Workshop, VIA platform, 6-10 July 2020

Comparison with MHD turbulence

S. Huber, T. Konstandin 2008

Criteria for phase transitions I

Vacuum bubbles nucleated from first order phase transitions (FOPT)

Three sources of GW production: 1) collision, 2) sound waves and 3) plasma turbulence

$h^2\Omega_{\text{col}}$ dominates for large wall velocities $v_b \to 1$

$$h^2\Omega\left(f;\,\alpha,\,\beta/H,f_{\text{peak}}\right) \qquad f_{\text{peak}}\left(\alpha,\,\beta/H,\,T_n\right)$$

$$\alpha \propto \frac{1}{T_n^4}\left[V_i - V_f - T\left(\frac{\partial V_i}{\partial T} - \frac{\partial V_f}{\partial T}\right)\right] \qquad \frac{\beta}{H} = T_n\frac{\partial}{\partial T}\left(\frac{\hat{S}_3}{T}\right)\bigg|_{T_n}$$

Criteria for phase transitions II

Bubble nucleation arises when the probability to realize 1 transition per cosmological horizon is equal to one: $\frac{\Gamma}{H^4} \sim 1 \implies \frac{\hat{S}_3}{T_n} \sim 140$

Strong transition criterion: $\frac{v_h(T_n)}{T_n} \geq 1 \implies$ enhances GW production

Classical motion in Euclidean space described by action $\hat{S}^3$

$$\hat{S}_3 = 4\pi \int_0^\infty dr\, r^2 \left\{ \frac{1}{2} \left(\frac{d\hat{\phi}}{dr} \right)^2 + V_{\text{eff}}(\hat{\phi}, T) \right\}$$

$$V_{\text{eff}}^{(1)}(\hat{\phi}, T) = V_0 + V_{\text{CW}} + \Delta V^{(1)}(T)$$

solution of the e.o.m. found by the path that minimizes the energy

Implementation via CosmoTransitions [Wainwright '12]

XXIII Bled (Virtual) Workshop, VIA platform, 6-10 July 2020

Dynamics of phase transitions

$$\Gamma \sim T^4 \left(\frac{\hat{S}_3}{2\pi T} \right)^{3/2} \exp \left(-\frac{\hat{S}_3}{T} \right)$$

High $T \Rightarrow$ classical motion in Euclidean space described by the action

$$\hat{S}_3 = 4\pi \int_0^\infty dr \, r^2 \left\{ \frac{1}{2} \left(\frac{d\hat{\phi}}{dr} \right)^2 + V_{\text{eff}}(\hat{\phi}) \right\}$$

Field configuration as solutions to the e.o.m. found by the path that minimizes the energy

$$V_{\text{eff}}^{(1)}(\hat{\phi}) = V_{\text{tree}} + V_{\text{CW}} + \Delta V^{(1)}(T)$$

$$V_{\text{CW}} = \sum_i (-1)^F n_i \frac{m_i^4}{64\pi^2} \left(\log \left[\frac{m_i^2(\hat{\phi}_\alpha)}{\Lambda^2} \right] - c_i \right)$$

$$\Delta V^{(1)}(T) = \frac{T^4}{2\pi^2} \left\{ \sum_b n_b J_B \left[\frac{m_b^2(\hat{\phi}_\alpha)}{T^2} \right] - \sum_f n_f J_F \left[\frac{m_f^2(\hat{\phi}_\alpha)}{T^2} \right] \right\}$$

Loop and thermal corrections in then effective potential

XXIII Bled (Virtual) Workshop, VIA platform, 6-10 July 2020

Time-crystal ground state and production of GW from QCD phase transitions

Some features of QCD

Different domains: from neutron stars equation of states and mergings, to colliders physics (proton-proton and heavy ions collisions)

SSB & dimensional trans-mutation: SSB, chiral anomaly and strong CP problem, and anomaly of the conformal symmetry and emergence of the QCD scale

Un-trivial ground states: inhomogeneous vacuum state with emergence of structure below the Fermi scale

Dynamics of the ground state: the appearance of condensate dynamically breaks the Lorentz symmetry

Confinement and the ground state dynamics: can we gain inspiration and suggestion from cosmology to progress towards the resolution of this problem?

Time-crystals I

Time-crystals: non-isolated matter, in non-equilibrium dynamics, shows periodic patterns not only in space, but also in time (Wilczek '12)

Quantum Time Crystals

Frank Wilczek

Center for Theoretical Physics Department of Physics, Massachusetts Institute of Technology, Cambridge, Massachusetts 02139, USA
(Received 29 March 2012; published 15 October 2012)

Some subtleties and apparent difficulties associated with the notion of spontaneous breaking of time-translation symmetry in quantum mechanics are identified and resolved. A model exhibiting that phenomenon is displayed. The possibility and significance of breaking of imaginary time-translation symmetry is discussed.

Time Crystals II

*"In a delicate balance between strong interactions, weak disorder, and a periodic driving force, a collection of trapped ions qubits has been made to pulsate with a period that is relatively insensitive to the drive. This is a **time crystal**, where the stable pulses emerge and break time symmetry – just like a freezing liquid breaks spatial symmetry and forms a spatial crystal. Trapped ion qubits can pulsate on their own with excellent passive stability, but this observation may guide the stabilization of complex solid-state systems, where true quantum behavior is usually masked by defects and impurities."*

In 2016 Monroe's group at Maryland University trapped a chain 171Yb+ (Ytterbium) ions in a Paul trap, a radio frequency device that uses e.m. dynamic to trap charged particles.

Among the two spin states, one is selected by a pair of laser beams. The shape of the lasers' pulse was controlled by an acousto-optic modulator.

A Tukey window was used to avoid that a critical amount of energy would have been peaked at the resonant optical frequency.

Time Crystals III

The hyperfine electron states in the setup used have very close energy levels, which are separated by 12.642831 GHz.

Finally, ten Doppler-cooled ions are placed in a line 25 µm long, and are coupled together.

Researchers observed subharmonic oscillations of the drive, with "rigidity" of the time crystal, and its oscillation frequency unchanged even under perturbation of the time crystal.

Once the perturbation or the frequency of the vibration grows too strong, the time crystal "melts".

Time-crystals and the Dynamical Universe

Time-crystals cannot be in equilibrium

Matter in non-equilibrium in its ground state!

Reminiscent of QCD, but can it be realized in the Universe?

Can a gluon condensate form, because of the space-time backreaction, which shows a time-crystal behavior?

This traces back to question about QCD relaxation phenomena that are related

Coupled YM-Einstein equations I

Incorporate the conformal anomaly via the variational procedure

The gauge coupling gYM should acquire a dependence on the quantum fields (RG eqs.)

$$\mathcal{L}_{\text{eff}} = \frac{\mathcal{J}}{4\bar{g}^2}, \quad \bar{g}^2 = \bar{g}^2(\mathcal{J}), \quad \mathcal{J} = -\frac{\mathcal{F}^a_{\mu\nu}\mathcal{F}^{\mu\nu}_a}{\sqrt{-g}}$$

$$g_{\mu\nu} = a(\eta)^2 \text{diag}(1, -1, -1, -1)$$

$$\mathcal{J} = \frac{2}{\sqrt{-g}} \sum_a (\mathbf{E}_a \cdot \mathbf{E}_a - \mathbf{B}_a \cdot \mathbf{B}_a) \equiv \frac{2}{\sqrt{-g}} (\mathbf{E}^2 - \mathbf{B}^2)$$

Chromoelectric (chromomagnetic) contributions contribute with positive (negative) sign to the energy density

Coupled YM-Einstein equations II

A. Addazi, A. Marciano, R. Pasechnik & G. Prokorov, EPJC '19

The gauge coupling satisfies the RG equation

$$2\mathcal{J}\frac{d\bar{g}^2}{d\mathcal{J}} = \bar{g}^2\beta$$

Starting from the effective action, one recover at the all-loop the effective YM eom, supplemented by the RG equation

$$\vec{\mathcal{D}}_\nu^{ab}\left[\frac{\mathcal{F}_b^{\mu\nu}}{\bar{g}^2\sqrt{-g}}\left(1 - \frac{\beta(\bar{g}^2)}{2}\right)\right] = 0 \qquad \frac{d\ln|\bar{g}^2|}{d\ln|\mathcal{J}|/\mu_0^4} = \frac{\beta(\bar{g}^2)}{2}$$

$$\vec{\mathcal{D}}_\nu^{ab} \equiv \left(\delta^{ab}\frac{\vec{\partial}_\nu\sqrt{-g}}{\sqrt{-g}} - f^{abc}\mathcal{A}_\nu^c\right)$$

Coupled YM-Einstein equations III

A. Addazi, A. Marciano, R. Pasechnik & G. Prokorov, EPJC '19

EMT for the Savvidy's theory

$$T_\mu^\nu = \frac{1}{\bar{g}^2}\left[\frac{\beta(\bar{g}^2)}{2} - 1\right]\left(\frac{\mathcal{F}_{\mu\lambda}^a \mathcal{F}_a^{\nu\lambda}}{\sqrt{-g}} + \frac{1}{4}\delta_\mu^\nu \mathcal{J}\right) - \delta_\mu^\nu \frac{\beta(\bar{g}^2)}{8\bar{g}^2}\mathcal{J}$$

Chromoelectric vacuum contributions to EMT

$$T_\mu^\mu = -\frac{\beta(\bar{g}_*^2)}{2\bar{g}_*^2}\mathcal{J}^* = -\frac{1}{\bar{g}_*^2}\mathcal{J}^*$$

Chromomagnetic vacuum contributions to EMT

$$T_\mu^\nu = \frac{-2}{\bar{g}^2}\left(\frac{\mathcal{F}_{\mu\lambda}^a \mathcal{F}_a^{\nu\lambda}}{\sqrt{-g}} + \frac{1}{4}\delta_\mu^\nu \mathcal{J}^*\right) - \delta_\mu^\nu \frac{\beta(\bar{g}_*^2)}{8\bar{g}_*^2}\mathcal{J}^* \qquad \longrightarrow \qquad T_\mu^\mu = \frac{1}{\bar{g}_*^2}\mathcal{J}^*$$

Coupled YM-Einstein equations IV

The coupled YM-Einstein equations read

$$\frac{1}{\varkappa}\left(R_\mu^\nu - \frac{1}{2}\delta_\mu^\nu R\right) = \bar{\epsilon}\delta_\mu^\nu + \frac{b}{32\pi^2}\frac{1}{\sqrt{-g}}\left[\left(-\mathcal{F}_{\mu\lambda}^a\mathcal{F}_a^{\nu\lambda}\right.\right.$$

$$\left.+ \frac{1}{4}\delta_\mu^\nu\mathcal{F}_{\sigma\lambda}^a\mathcal{F}_a^{\sigma\lambda}\right)\ln\frac{e|\mathcal{F}_{\alpha\beta}^a\mathcal{F}_a^{\alpha\beta}|}{\sqrt{-g}\,\lambda^4} - \frac{1}{4}\delta_\mu^\nu\,\mathcal{F}_{\sigma\lambda}^a\mathcal{F}_a^{\sigma\lambda}\Bigg],$$

$$\left(\frac{\delta^{ab}}{\sqrt{-g}}\vec{\partial}_\nu\sqrt{-g} - f^{abc}\mathcal{A}_\nu^c\right)\left(\frac{\mathcal{F}_b^{\mu\nu}}{\sqrt{-g}}\ln\frac{e|\mathcal{F}_{\alpha\beta}^a\mathcal{F}_a^{\alpha\beta}|}{\sqrt{-g}\,\lambda^4}\right) = 0$$

On FLRW backgrounds
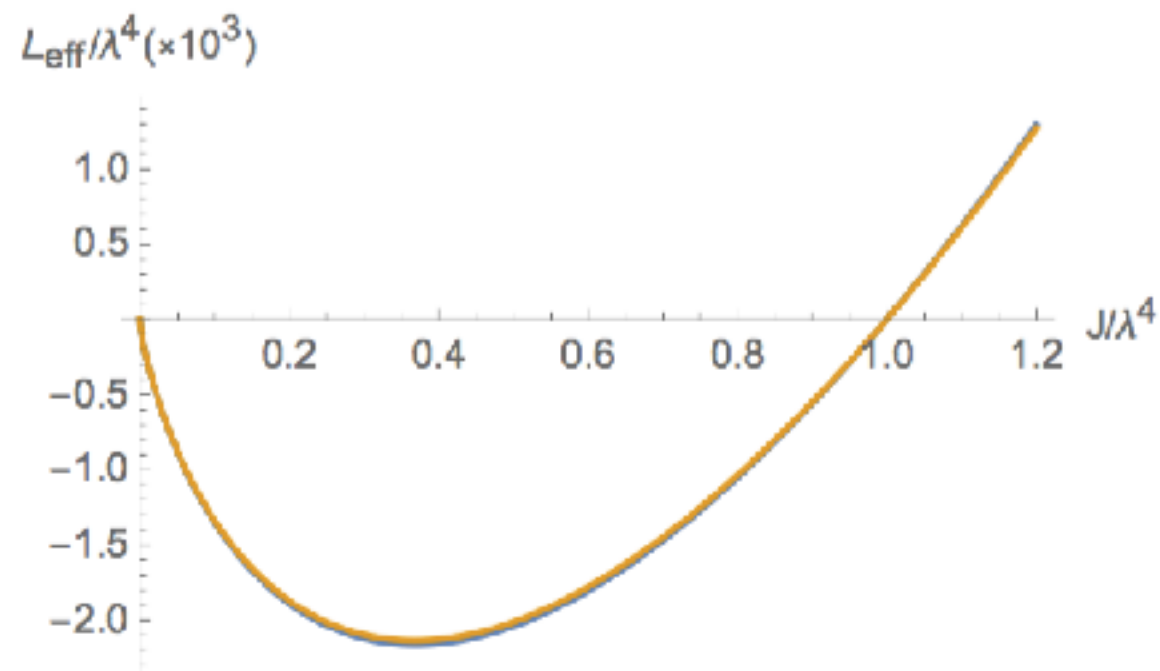
$$\frac{3}{\varkappa}\frac{(a')^2}{a^4} = \bar{\epsilon} + T_0^{0,\mathrm{U}},$$

$$T_0^{0,\mathrm{U}} = \frac{3b}{64\pi^2 a^4}\left(\left[(U')^2 + \frac{1}{4}U^4\right]\ln\frac{6e|(U')^2 - \frac{1}{4}U^4|}{a^4\lambda^4}\right.$$

$$\left.+ (U')^2 - \frac{1}{4}U^4\right).$$

$$\frac{6}{\varkappa}\frac{a''}{a^3} = 4\bar{\epsilon} + T_\mu^{\mu,\mathrm{U}},$$

$$T_\mu^{\mu,\mathrm{U}} = \frac{3b}{16\pi^2 a^4}\left[(U')^2 - \frac{1}{4}U^4\right],$$

$$\frac{\partial}{\partial\eta}\left(U'\ln\frac{6e|(U')^2 - \frac{1}{4}U^4|}{a^4\lambda^4}\right)$$

$$+ \frac{1}{2}U^3\ln\frac{6e|(U')^2 - \frac{1}{4}U^4|}{a^4\lambda^4} = 0$$

One-loop effective action

The standard one-loop SU(N) beta-function reads

G. Savvidy, PLB '77

$$\beta_1 = -\frac{bN}{48\pi^2}\,\bar{g}_1^2\,, \qquad b = 11$$

$$\bar{g}_1^2(\mathcal{J}) = \frac{\bar{g}_1^2(\mu_0^4)}{1 + \frac{bN}{96\pi^2}\bar{g}_1^2(\mu_0^4)\ln(|\mathcal{J}|/\mu_0^4)}$$

$$\mathcal{L}_{\text{eff}}^{(1)} = \frac{bN}{384\pi^2}\,\mathcal{J}\ln\left(\frac{|\mathcal{J}|}{\lambda^4}\right)$$

Beyond one-loop effective action I

The all-loops effective action of SU(2) YM theory predicted by the FRG approach

P. Dona, A. Marciano, Y. Zhang & C. Antolini, PRD '16

$$\mathcal{L}_{\text{eff}} = \frac{2\,\mathcal{J}}{16\pi^2} \int_0^\infty \frac{ds}{s} \left[e^{-s\sqrt{\frac{\lambda^4}{\mathcal{J}\tanh(\mathcal{J}/\lambda^4\varepsilon)}}} - e^{-s} \right]$$

$$\times \left[\frac{1}{4\sinh^2 s} - \frac{1}{4s^2} + 1 \right], \quad \varepsilon \ll 1,$$

$$\downarrow$$

$$\mathcal{J}\tanh\left(\frac{\mathcal{J}}{\varepsilon\lambda^4}\right)\Big|_{\varepsilon\to 0} \to |\mathcal{J}|$$

Corresponding all-loops coupling constant

$$[\bar{g}^2]^{-1} = \frac{2}{4\pi^2} \int_0^\infty \frac{ds}{s} \left[e^{-s\sqrt{\frac{\lambda^4}{\mathcal{J}\tanh(\mathcal{J}/\varepsilon\lambda^4)}}} - e^{-s} \right]$$

$$\times \left[\frac{1}{4\sinh^2 s} - \frac{1}{4s^2} + 1 \right]$$

Beyond one-loop effective action II

The all-loops effective action of SU(2) YM theory predicted by the FRG approach

$$\frac{\beta}{\bar{g}^2} = \frac{-1}{2\pi^2}\sqrt{\frac{\lambda^4}{\mathcal{J}\tanh(\mathcal{J}/\varepsilon\lambda^4)}}\int_0^\infty ds\, e^{-s\sqrt{\frac{\lambda^4}{\mathcal{J}\tanh(\mathcal{J}/\varepsilon\lambda^4)}}}$$

$$\times \left[\frac{1}{4\sinh^2 s} - \frac{1}{4s^2} + 1\right],$$

$$s \to 0$$

$$\ln A = \int_0^\infty \frac{ds}{s}\left[e^{-sA} - e^{-s}\right], \qquad A > 0$$

$$\left[\frac{1}{4\sinh^2 s} - \frac{1}{4s^2} + 1\right] = \frac{11}{12} + \mathcal{O}(s^2)$$

the exact form of the one-loop effective action is recovered

XXIII Bled (Virtual) Workshop, VIA platform, 6-10 July 2020

Vanishing gravitational effects

The spatially and homogenous isotropic part of A satisfies the classical YM eom

$$(\dot{U})^2 + \bar{g}^2 \, U^4 = \text{const}$$

integrated analytically in terms of Jacobi Elliptic functions

$$U(t) = U_0 \, |\text{cd}(\bar{g}U_0 t| - 1)| \,,$$
$$U(0) = U_0 > 0 \,, \qquad \dot{U}(0) = 0$$

oscillatory quasi-harmonic function in time

$$U(n \, T_U) = U_0 \,, \quad U\left(\left(n + \frac{1}{4}\right) T_U\right) = 0 \,, \quad n = 0, 1, 2, \ldots$$

$$U_0 > 0 \qquad T_U = B\left(\frac{1}{4}, \frac{1}{2}\right)(\bar{g}U_0)^{-1} \simeq 1.2 \times \pi(\bar{g}U_0)^{-1}$$

The case of SU(3)

A. Addazi, A. Marciano, R. Pasechnik & G. Prokorov, EPJC '19

$$A_k = A_{ak}\frac{\lambda_a}{2}, \qquad \left[\frac{\lambda_a}{2}, \frac{\lambda_b}{2}\right] = if_{abc}\frac{\lambda_c}{2} \qquad a = 1,\dots,8$$

A special minimal su(2) algebra embedding into the su(3) in terms of three Gell-Mann matrices $\{\lambda 7, -\lambda 5, \lambda 2\}$

$$A_{ak} = (\delta_{a,7}\delta_{k,1} - \delta_{a,5}\delta_{k,2} + \delta_{a,2}\delta_{k,3})U(t) + \widetilde{A}_{ak}$$

$$\widetilde{A}_{ak} = \widetilde{A}_{ak}(t, \mathbf{x})$$

Again, in the absence of gravity, the spatially homogeneous/isotropic gluon condensate $U(t) > 0$ satisfies the classical YM eom

$$(\dot{U})^2 + \frac{1}{4}\bar{g}^2 U^4 = \text{const}$$

XXIII Bled (Virtual) Workshop, VIA platform, 6-10 July 2020
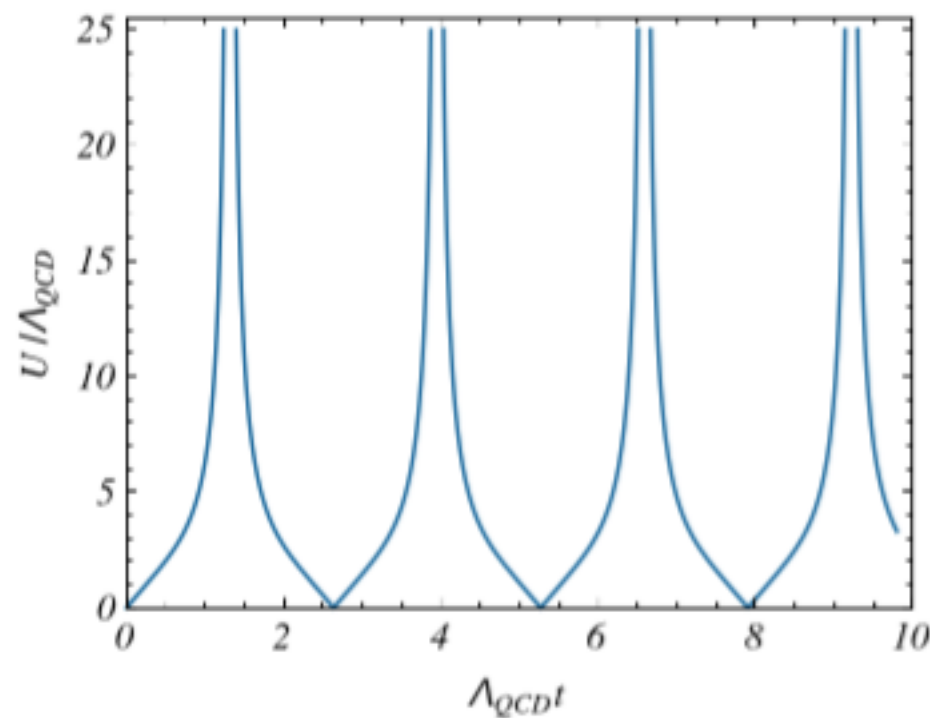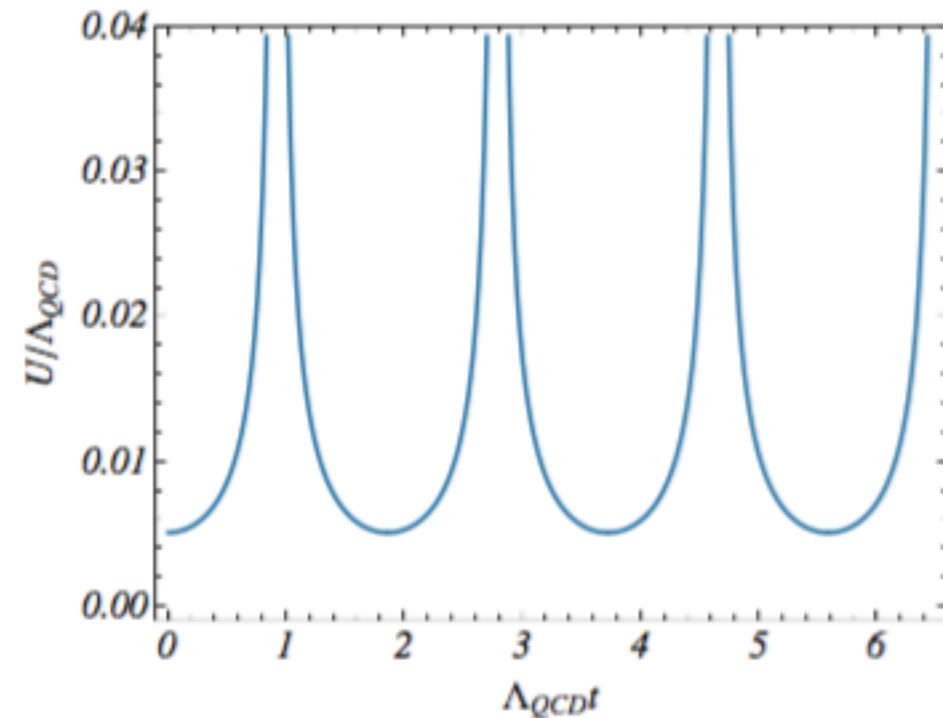
Savvidy vacua

A. Addazi, A. Marciano, R. Pasechnik & G. Prokorov, EPJC '19

Conventional Fock vacuum, empty of particles and fields, cannot apply to QCD

Solving for the Savvidy's theory for general asymptotic solutions

CE vacua

CM vacua

Time-crystal and pressure fluctuations

A. Addazi, A. Marciano, R. Pasechnik & G. Prokorov, EPJC '19

Solving numerically the YM-Einstein coupled system

Dissipative system, out of equilibrium: energy transferred to the primordial plasma

Translational-breaking and Kinks

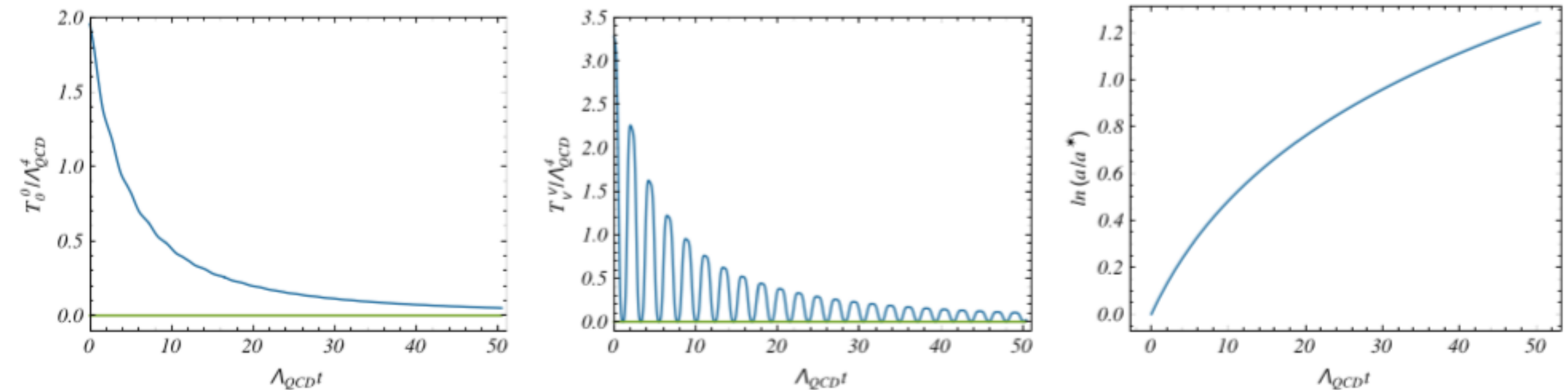Standard static domain-walls for a scalar field theory that is Z_2 invariant, and with sombrero-like Higgs potential

SSB of Z_2**:** when the scalar field rolls down to one of the two possible minima $\phi_{vac} = \pm v$

$$\phi(z) = v \tanh\left[\frac{\lambda v}{\sqrt{2}}(z - z_0)\right]$$

z0 kink center

The kink profile interpolating the two minima, when internal field configurations are localized in the space direction z

Translational invariance is spontaneously broken, being the barrier localized in a z0 point

Nambu-Goldstone modulus boson z0(t, x, y), localized on the surface of the domain wall, as a low energy-excitation of its surface in the z-direction

T-breaking and space-like domains I

A. Addazi, A. Marciano & R. Pasechnik, CPC '19

Consider a kink profile that, no more localized in a space direction, but in time

$$\phi(t) = v \tanh\left[\tfrac{\lambda v}{\sqrt{2}}(t - t_0)\right]$$

t_0 kink center

interpolating the two vacuum states in the asymptotic time limits

$$\phi(t = -\infty) = -v \qquad \phi(t = \infty) = v$$

This instantiates a SSB of the time invariance and triggers the appearance of a Nambu-Goldstone boson localized on the xyz surface t0(x, y, z)

T-breaking and space-like domains II

A. Addazi, A. Marciano & R. Pasechnik, CPC '19

Gluon condensate field equation coupled to gravity, in a FLRW background

Let us consider the limit of a static FLRW space time (a = const)

$$U'^2 - \frac{1}{4}U^4 = \text{const}$$

A branch of solutions of these equations, obtained by $U^2 \rightarrow U^2 - U_0^2$ energy density vacuum shift, corresponds to kink (anti-kink) profiles

$$U(\eta) \simeq \frac{v}{\sqrt{2}} \tanh[\frac{v}{\sqrt{2}}(\eta - \eta_0)] \qquad v \simeq \Lambda_{\text{QCD}}$$

A space-like domain wall corresponds to a kink profile of this type

T-breaking and space-like domains III

Time-translation is spontaneously broken, and a η0(x, y, z) moduli field arises, with U acquiring the dependence U(η − η0(x, y, z))

The coordinate x, y, z are the domain-walls worldsheet coordinates.

The effective corresponding action reads as

$$S = \int d^4x \, \frac{1}{2}\left[\left(\frac{\partial \phi}{\partial \eta_0}\frac{\partial \eta_0}{\partial x^a}\right)^2 - V(U)\right]$$

$$= \text{const} + \frac{T_W}{2}\int d^3x \left(\frac{\partial \eta_0(x^a)}{\partial x^a}\right)^2$$

The moduli field is massless, according to the Nambu-Goldstone theorem

T-breaking with gravitational dynamics I

When the scale factor time-dependence is considered, a more complicated time pattern for the space-like domain walls arises

Time-translation is spontaneously broken down to a discrete time-translation symmetry:
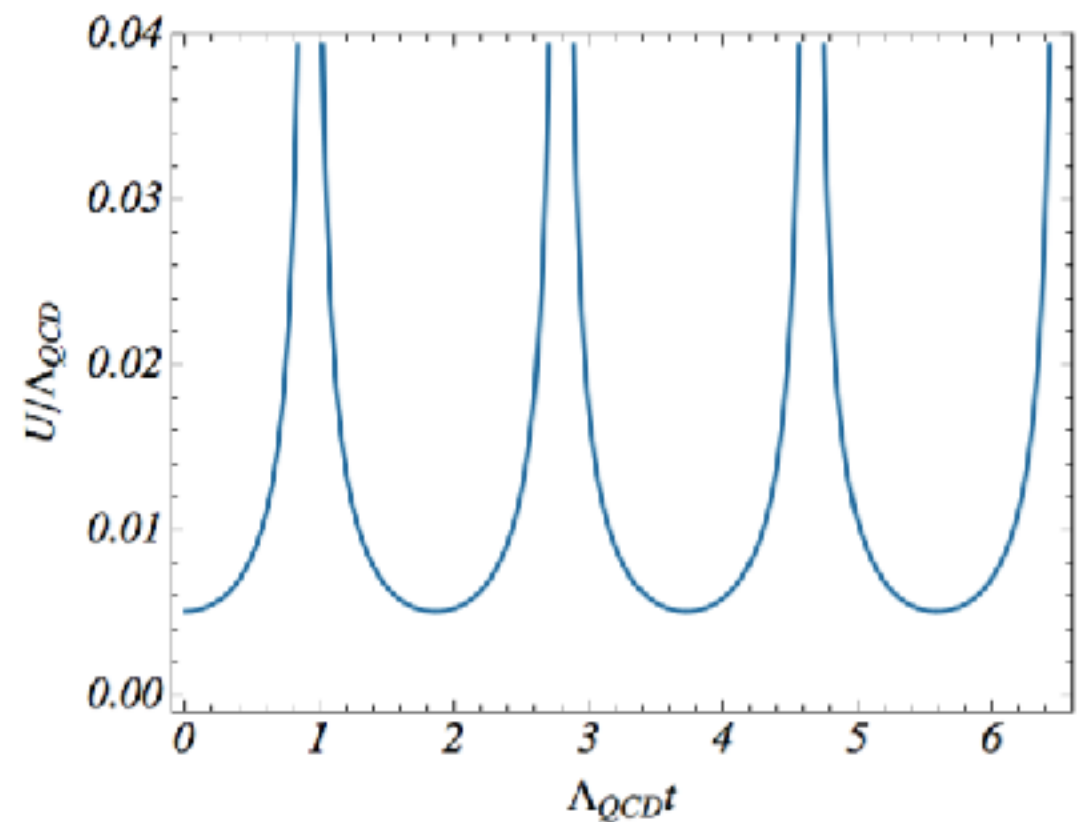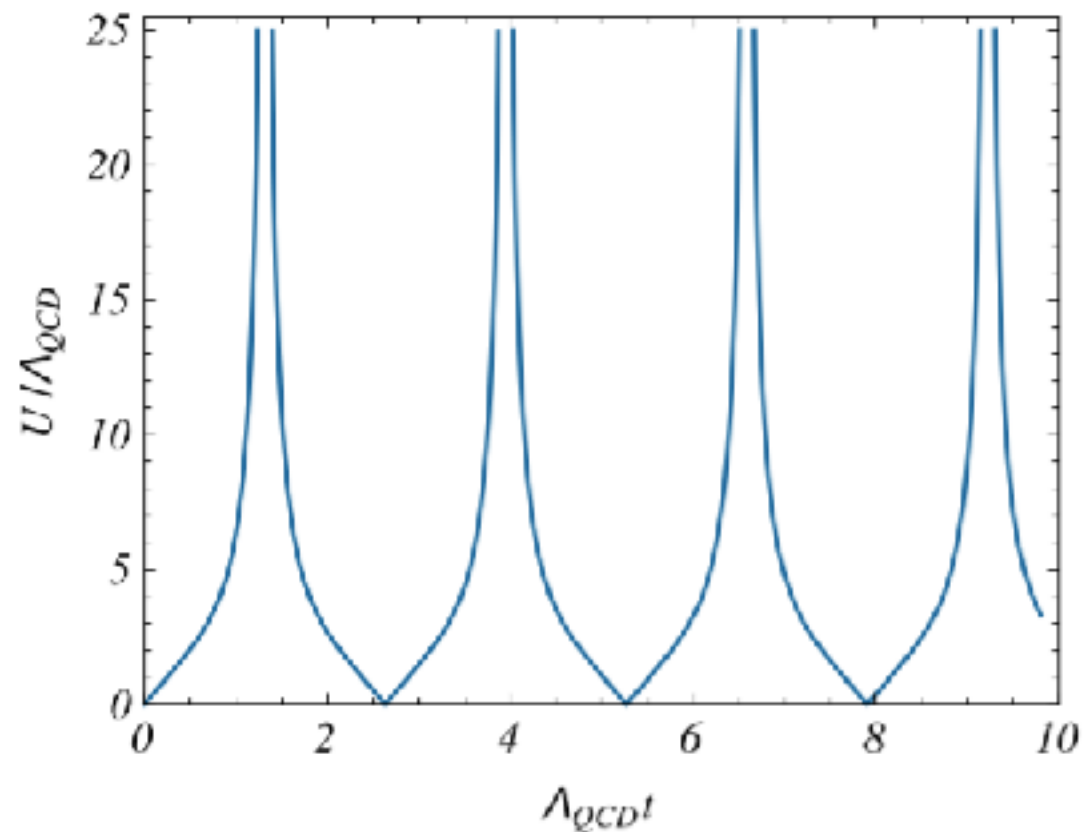
$$T_n : \eta \to \eta + n\Lambda_{\text{QCD}}^{-1}$$

T-breaking with gravitational dynamics II

A. Addazi, A. Marciano & R. Pasechnik, CPC '19
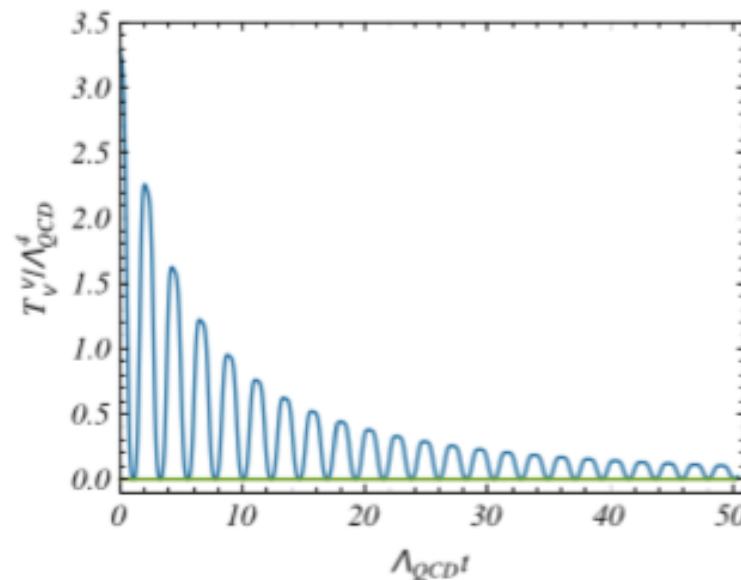
$$T_n : \eta \to \eta + n\Lambda_{\mathrm{QCD}}^{-1}$$

The system behaves as a time-crystal!

Any way to compare with lattice QCD?

Can Lattice QCD capture this dynamical and non-perturbative regime?

Can we slice FLRW with Minkowski in a time range much smaller than $\Lambda_{\text{QCD}}^{-1}$?
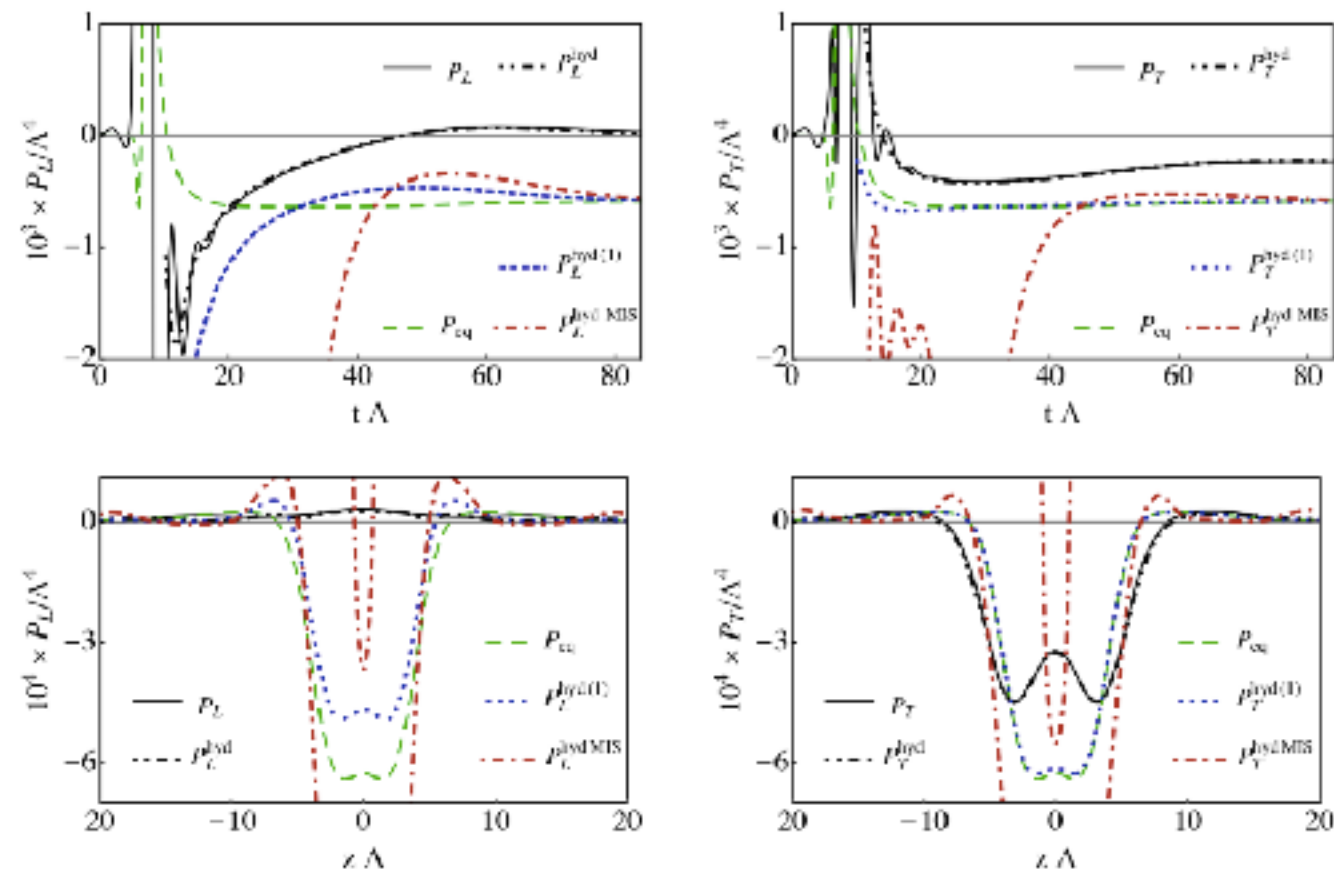
Validity of Wick rotation and equilibrium dynamics in the Euclidean!

Maiani-Testa theorem (PLB '90): scattering for asymptotic states can be counter-Wick rotated only in the infinite volume limit (the scale being the threshold amplitude) and for time much smaller than the level spacing due to momentum discretization

XXIII Bled (Virtual) Workshop, VIA platform, 6-10 July 2020

Comparison with QCD holography*

M. Attems, Y. Bea, J. Casalderrey-Solana, D. Mateos, M. Triana & M. Zilhão, PRL '18

"Holography to analyze relativistic collisions in a one-parameter family of strongly coupled gauge theories with thermal phase transitions"

But conclude that "out-of-equilibrium physics smooths out the details of the transition"

Not only an academic issue: we ask Nature

A. Addazi, A. Marciano & R. Pasechnik, CPC '19
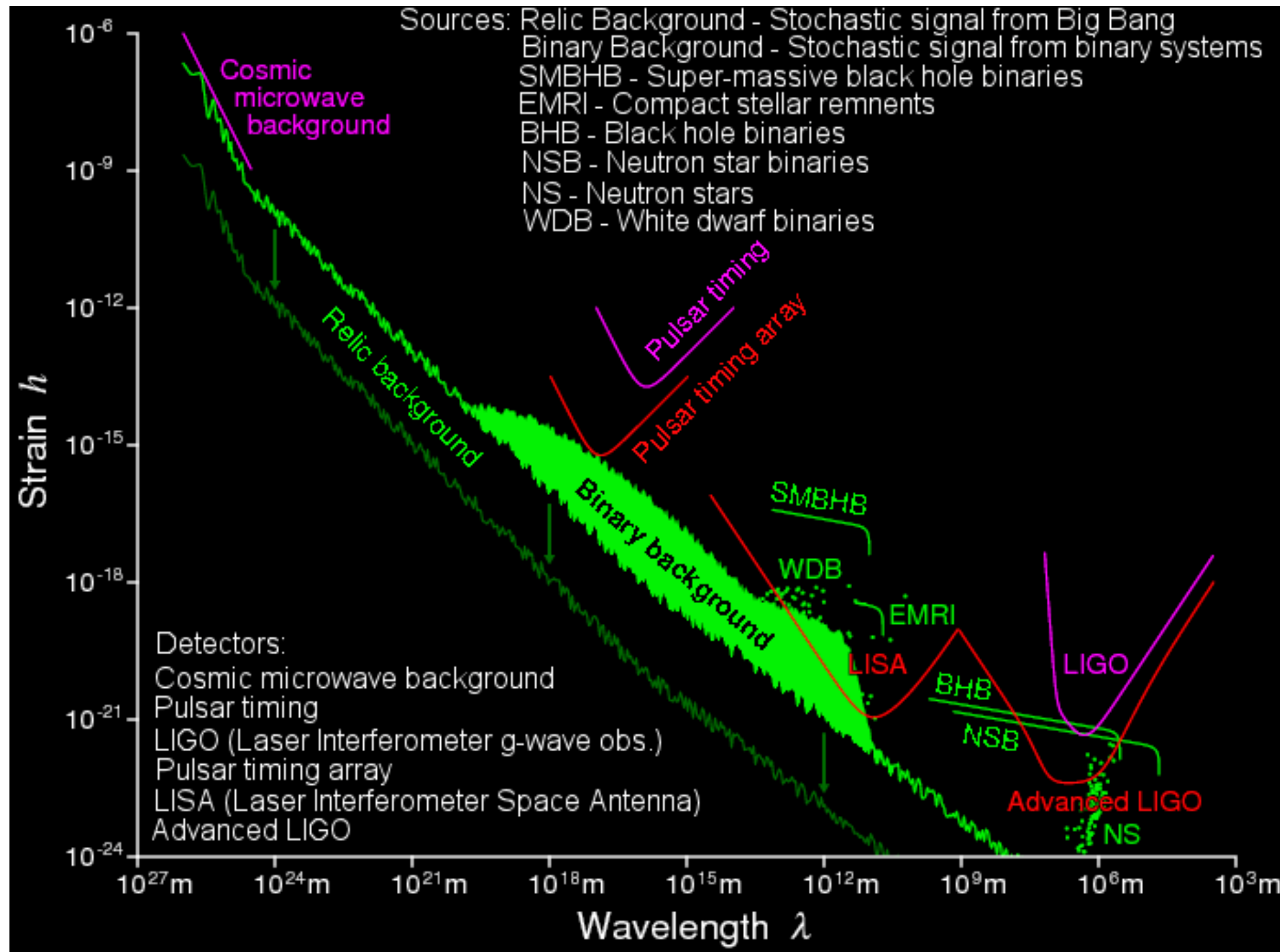
Is there any observable that makes falsifiable this insight?

Pressure oscillations start at a time related to the QCD scale, and are after few cycles suppressed

This effect might leave an imprinting on the primordial plasma, generating GWs in the nHz domains, so within the radio-frequency range of Pulsars Timing

Turbulence and sounds waves shall be taken into account as GW sources

XXIII Bled (Virtual) Workshop, VIA platform, 6-10 July 2020

GW frequencies domain

Primordial plasma and GWs

A. Addazi, A. Marciano & R. Pasechnik, CPC '19

$$\alpha = \frac{\rho_U}{\rho_{\mathrm{rad}}}$$ latent energy released by the gluon condensate into the primordial plasma

$$\beta_i \simeq \Lambda$$ inverse time scale of the peaks, related to the inverse of the QCD scale

Redshifts factors must be taken into account

$$\frac{R_*}{R_0} = 8.0 \times 10^{-14} \left(\frac{100}{g_*}\right)^{\frac{1}{3}} \left(\frac{1\,\mathrm{GeV}}{T_*}\right)$$

$$f_0 = f_* \left(\frac{R_*}{R_0}\right) = 1.65 \times 10^{-7}\,\mathrm{Hz} \left(\frac{f_*}{H_*}\right) \left(\frac{T_*}{1\,\mathrm{GeV}}\right) \left(\frac{g_*}{100}\right)^{\frac{1}{6}}$$

$$H_* = \frac{8\pi G \rho_{\mathrm{rad}}}{3} = \frac{8\pi^3 g_* T_*^4}{90 M_{Pl}^2} \qquad \Omega_{\mathrm{GW}} = \Omega_{\mathrm{GW}*} \left(\frac{R_*}{R_0}\right)^4 \left(\frac{H_*}{H_0}\right)^2$$

Sounds waves and turbulences effects

A. Addazi, A. Marciano & R. Pasechnik, CPC '19

$$h^2\Omega_{\text{turb}} = 3.35 \times 10^{-4} \sum_i^{N_{\text{eff}}} \left(\frac{H_{*,i}}{\beta_i}\right)\left(\frac{\kappa_{turb}\alpha}{1+\alpha}\right)^{\frac{3}{2}}\left(\frac{100}{g_{*,i}}\right)^{\frac{1}{3}} v,$$

$$f_{\text{turb}} = 2.7 \times 10^{-2}\,\text{mHz}\frac{1}{v}\left(\frac{\beta_i}{H_{*,i}}\right)\left(\frac{E_{*,i}}{\text{GeV}}\right)\left(\frac{g_{*,i}}{100}\right)^{\frac{1}{6}}$$

$$h^2\Omega_{\text{sound}} = 2.65 \times 10^{-6} \sum_{i=1}^{N_{\text{eff}}} \left(\frac{H_{*,i}}{\beta_i}\right)\left(\frac{\kappa_v\alpha}{1+\alpha}\right)^{2}\left(\frac{100}{g_{*,i}}\right)^{\frac{1}{3}} v_i,$$

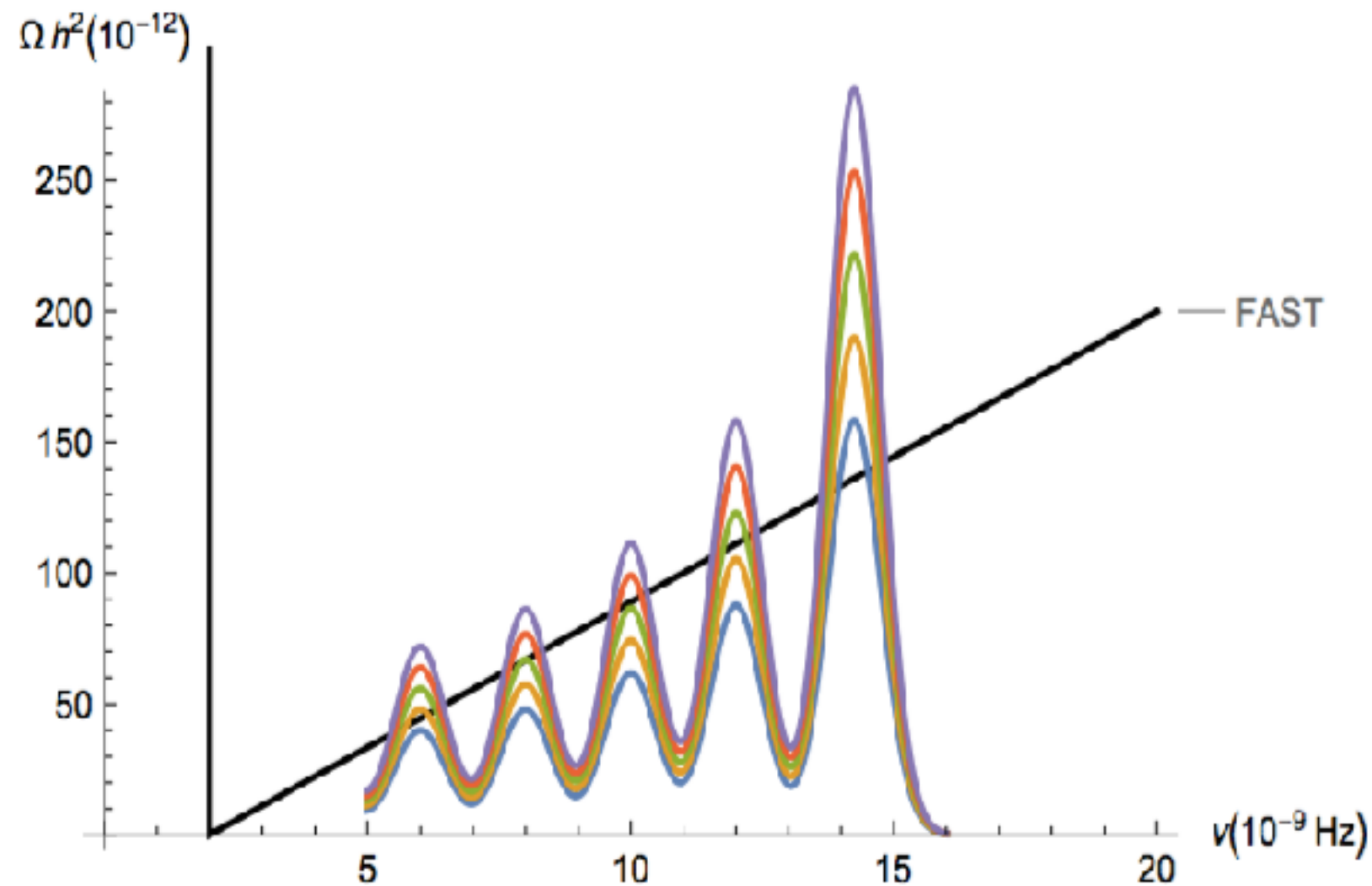$$f_{\text{sw}} = 1.9 \times 10^{-2}\text{mHz}\sum_{i=1}^{N_{\text{eff}}} \frac{1}{v_i}\left(\frac{\beta_i}{H_{*,i}}\right)\left(\frac{T_{*,i}}{100\,\text{GeV}}\right)\left(\frac{g_{*,i}}{100}\right)^{\frac{1}{6}}$$

Comparison with FAST sensitivity curves

A. Addazi, A. Marciano & R. Pasechnik, CPC '19

The GWs spectrum is displayed for different efficiency factors, in comparison with FAST sensitivity curve. The efficiency factor considered are $\kappa = 0.03 \div 0.1$

XXIII Bled (Virtual) Workshop, VIA platform, 6-10 July 2020

Comparison with SKA sensitivity curves
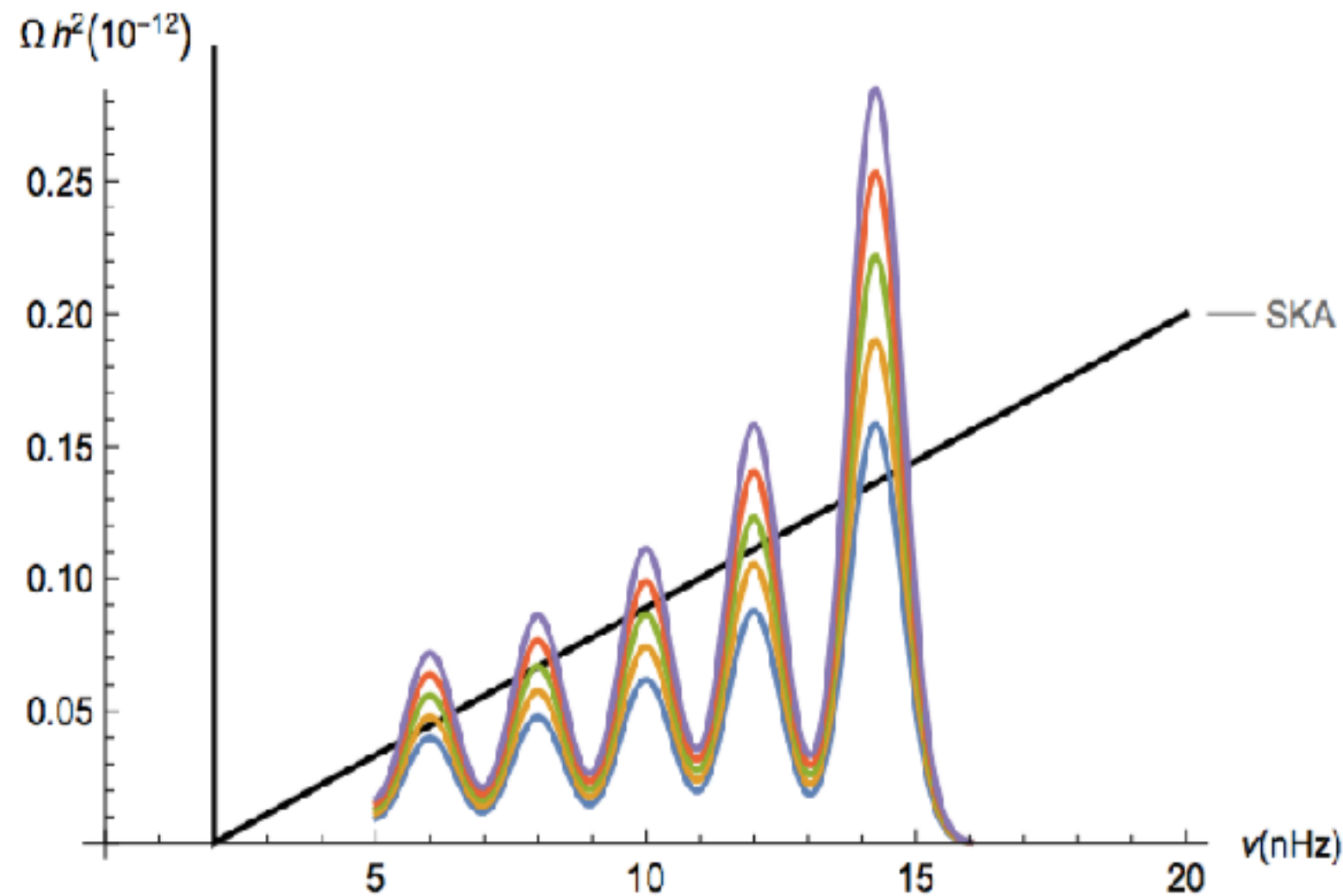
A. Addazi, A. Marciano & R. Pasechnik, CPC '19

The GWs spectrum is displayed for different efficiency factors, in comparison with SKA sensitivity curve. The efficiency factor considered are $\kappa = 0.001 \div 3 \times 0.001$

XXIII Bled (Virtual) Workshop, VIA platform, 6-10 July 2020

Neutrino physics and the mass-generation

XXIII Bled (Virtual) Workshop, VIA platform, 6-10 July 2020

Standard Type-I models (high scale)

$$\mathcal{L}_{\text{Yuk}}^{\text{Type}-I} = Y_\nu \bar{L} H \nu^c + M \nu^c \nu^c + h.c.$$

$L = (\nu, l)^T$ and ν^c three RH-neutrinos colored as SM-singlet

Y_ν and M 3 x 3 matrices

M explicitly break lepton number symmetry $U(1)_L \to \mathbb{Z}_2$

Mass for light neutrinos generated by EWSB $m_\nu \sim \mathcal{O}(0.1\text{eV})$

$$m_\nu^{\text{Type}-I} = \frac{v_h^2}{2} Y_\nu^T M^{-1} Y_\nu \qquad \langle H \rangle = \frac{v_h}{\sqrt{2}} \qquad Y_\nu \sim \mathcal{O}(1) \qquad M \sim O(10^{14}\text{GeV})$$

Inverse see-saw (low scale)

Two additional gauge singlet fermions, with opposite lepton number charge ν^c, S

$$\mathcal{L}_{\text{Yuk}}^{\text{Inverse}} = Y_\nu \bar{L} H \nu^c + M \nu^c S + \mu SS + \text{h.c.}$$

The smallness of the neutrino mass is linked to the breaking $U(1)_L \to \mathbb{Z}_2$

This is triggered by the μ-term $m_\nu^{\text{Inverse}} = \frac{v_h^2}{2} Y_\nu^T M^{T^{-1}} \mu M^{-1} Y_\nu$

Small neutrino masses are protected by $U(1)_L$ (restored for $\mu \to 0$)

Introducing the Majoron

Global B-L spontaneously broken by a SM complex scalar singlet and generation of LH neutrino mass

The NGB associated to the symmetry is the Majoron

Possible detection in neutrinoless double-beta decays (GERDA, EXO)

The effective action for the Majoron

$$\mathcal{L}_M = f H \bar{L} \nu_R + h \sigma \bar{\nu}_R \nu_R^c + h.c. + V(\sigma, H)$$

A complex singlet scalar σ, **the majoron**, with $L(\sigma) = -2$

$$V(\sigma, H) = V_0(\sigma, H) + V_1(\sigma) + V_2(h, \sigma)$$

$$V_0(\sigma, H) = \lambda_s \left(|\sigma|^2 - \frac{v_{BL}^2}{2} \right)^2 + \lambda_H \left(|H|^2 - \frac{v^2}{2} \right)^2$$
$$+ \lambda_{sH} \left(|\sigma|^2 - \frac{v_{BL}^2}{2} \right) \left(|H|^2 - \frac{v^2}{2} \right),$$

$$V_1(\sigma) = \frac{\lambda_1}{\Lambda} \sigma^5 + \frac{\lambda_2}{\Lambda} \sigma^* \sigma^4 + \frac{\lambda_3}{\Lambda} (\sigma^*)^2 \sigma^3 + h.c.$$

$$V_2(H, \sigma) = \beta_1 \frac{(H^\dagger H)^2 \sigma}{\Lambda} + \beta_2 \frac{(H^\dagger H) \sigma^2 \sigma^*}{\Lambda}$$
$$+ \beta_3 \frac{(H^\dagger H) \sigma^3}{\Lambda} + h.c..$$

The effective action for the Majoron

$$V_1^{(6)}(\sigma) = \frac{\gamma_1}{\Lambda^2}\sigma^6 + \frac{\gamma_2}{\Lambda^2}\sigma^*\sigma^5 + \frac{\gamma_3}{\Lambda^2}(\sigma^*)^2\sigma^4$$

$$+ \frac{\gamma_4}{\Lambda^2}(\sigma^*)^3\sigma^3 + h.c. \,,$$

$$V_2^{(6)}(\sigma, H) = \frac{\delta_1}{\Lambda^2}(H^\dagger H)^2\sigma^2 + \frac{\delta_2}{\Lambda^2}(H^\dagger H)^2\sigma^*\sigma$$

$$+ \frac{\delta_3}{\Lambda^2}(H^\dagger H)\sigma^3\sigma^* + \frac{\delta_4}{\Lambda^2}(H^\dagger H)(\sigma\sigma^*)^2$$

$$+ \frac{\delta_5}{\Lambda^2}(H^\dagger H)\sigma^4 + h.c. \,.$$

Z.G.Berezhiani, R.N.Mohapatra, G.Senjanovic, PRD 1993

Missing energy channel and LHC data

$$\Gamma(H \to \chi\chi) = \frac{C_{h\chi\chi}^2 v^2}{64\pi m_H} \sqrt{1 - \frac{m_\chi^2}{m_H^2}}$$

$$C_{H\chi\chi} = \lambda_{H\chi\chi} + \frac{\beta_2}{\Lambda} v_\sigma.$$

$$Br(H \to invisible) = \frac{\Gamma_{inv}}{\Gamma_{inv} + \Gamma_{SM}} < 0.51 \, (95\% \, \text{C.L.})$$

channel	ATLAS	CMS	ATLAS+CMS
$\mu_{\gamma\gamma}$	$1.15^{+0.27}_{-0.25}$	$1.12^{+0.25}_{-0.23}$	$1.16^{+0.20}_{-0.18}$
μ_{WW}	$1.23^{+0.23}_{-0.21}$	$0.91^{+0.24}_{-0.21}$	$1.11^{+0.18}_{-0.17}$
μ_{ZZ}	$1.51^{+0.39}_{-0.34}$	$1.05^{+0.32}_{-0.27}$	$1.31^{+0.27}_{-0.24}$
$\mu_{\tau\tau}$	$1.41^{+0.40}_{-0.35}$	$0.89^{+0.31}_{-0.28}$	$1.12^{+0.25}_{-0.23}$
μ_{bb}	$0.62^{+0.37}_{-0.36}$	$0.81^{+0.45}_{-0.42}$	$0.69^{+0.29}_{-0.27}$

$$\mu_F = \frac{\sigma^{NP}(pp \to H)}{\sigma^{SM}(pp \to H)} \frac{BR^{NP}(H \to F)}{BR^{SM}(H \to F)}$$

Majoron phenomenology

Cosmological limits very stringent on SSB scales beyond EW phase-transition

Very open limits on smaller scales!

Possibility to say something about the nature of the phase transition: violent Majoron, with FOPT

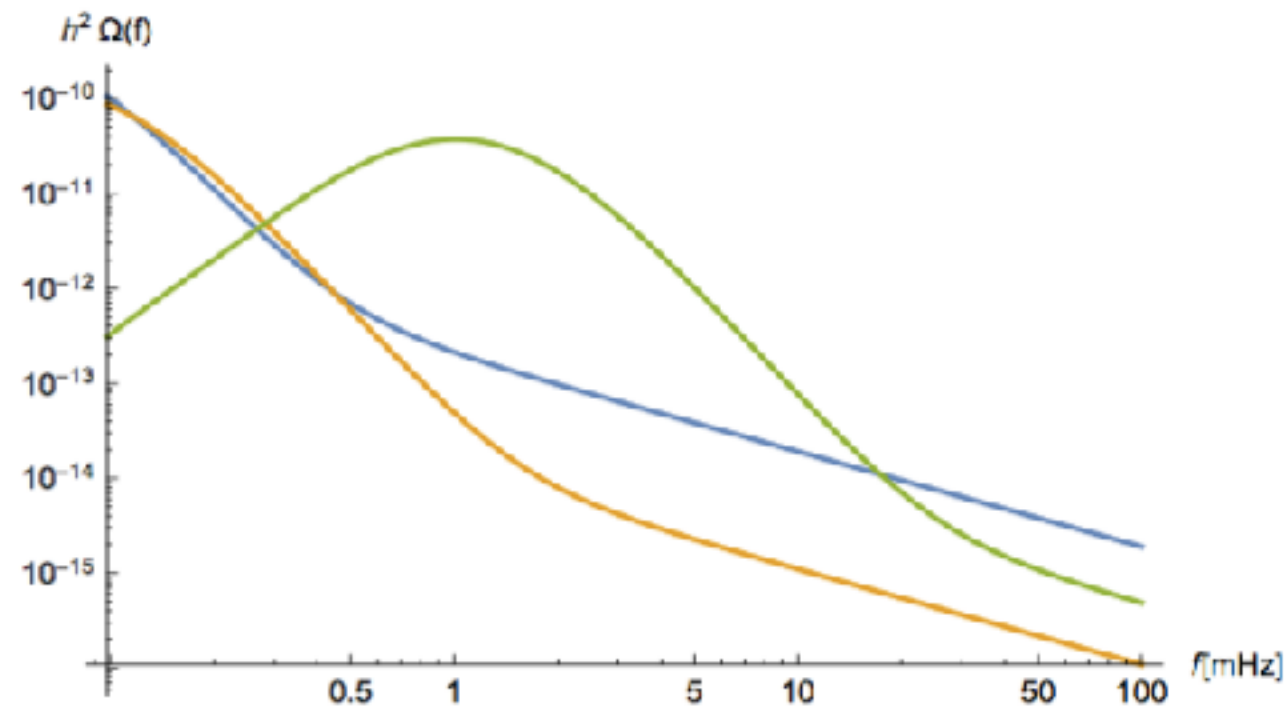A. Addazi & A. Marciano, CPC (2018), arXiv:1705.08346

FOPT at 10 GeV

FIG. 1. The gravitational waves energy density as a function of the frequency is displayed. We use the same model independent parametrization of Ref.[18]. We show three *non-runaway* bubbles cases which are compatible with the B-L first order phase transition: In blue, we consider the case of $\bar{T} = 50\,\text{GeV}$, $\beta/\bar{H} = 100$, $\alpha = 0.5$, $\alpha_\infty = 0.1$, $V_B = 0.95$; in green $\bar{T} = 20\,\text{GeV}$, $\beta/\bar{H} = 10$, $\alpha = 0.5$, $\alpha_\infty = 0.1$, $V_B = 0.95$. Orange: $\bar{T} = 10\,\text{GeV}$, $\beta/\bar{H} = 10$, $\alpha = 0.5$, $\alpha_\infty = 0.1$, $V_B = 0.3$. The three cases lies in the sensitivity range of LISA [18].

Constrained from GW, colliders and cosmology

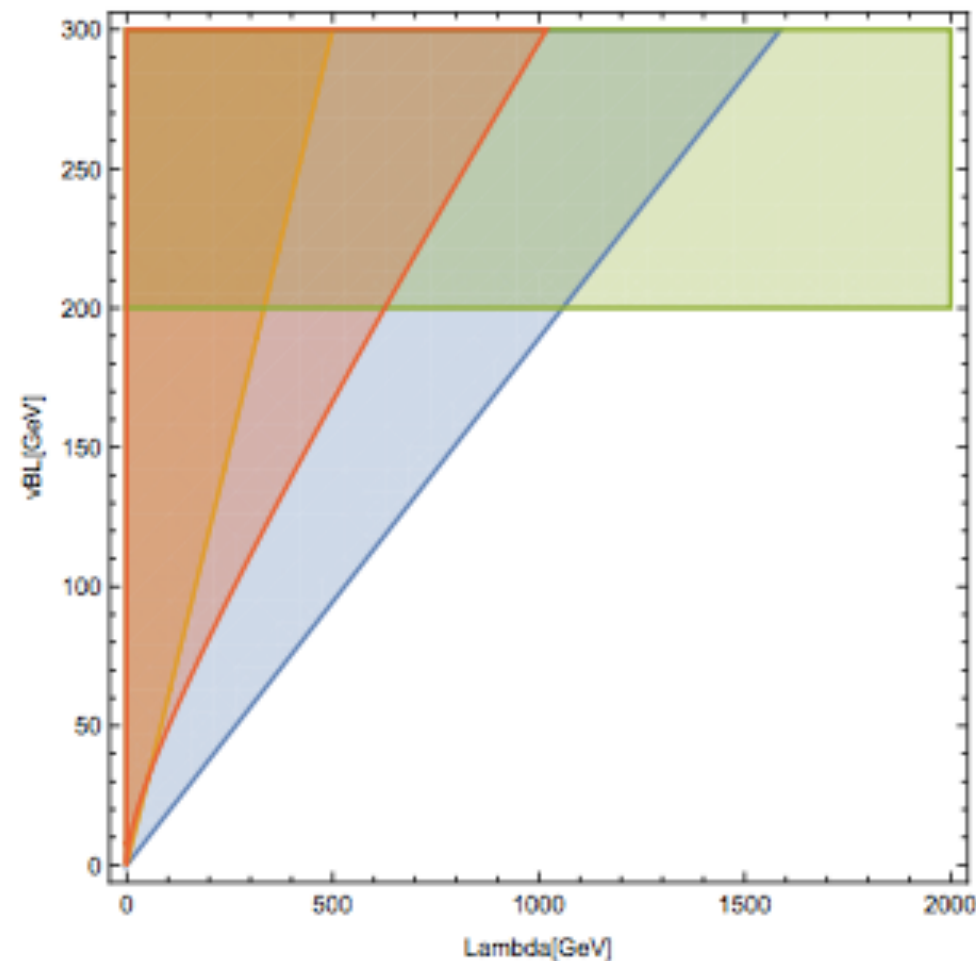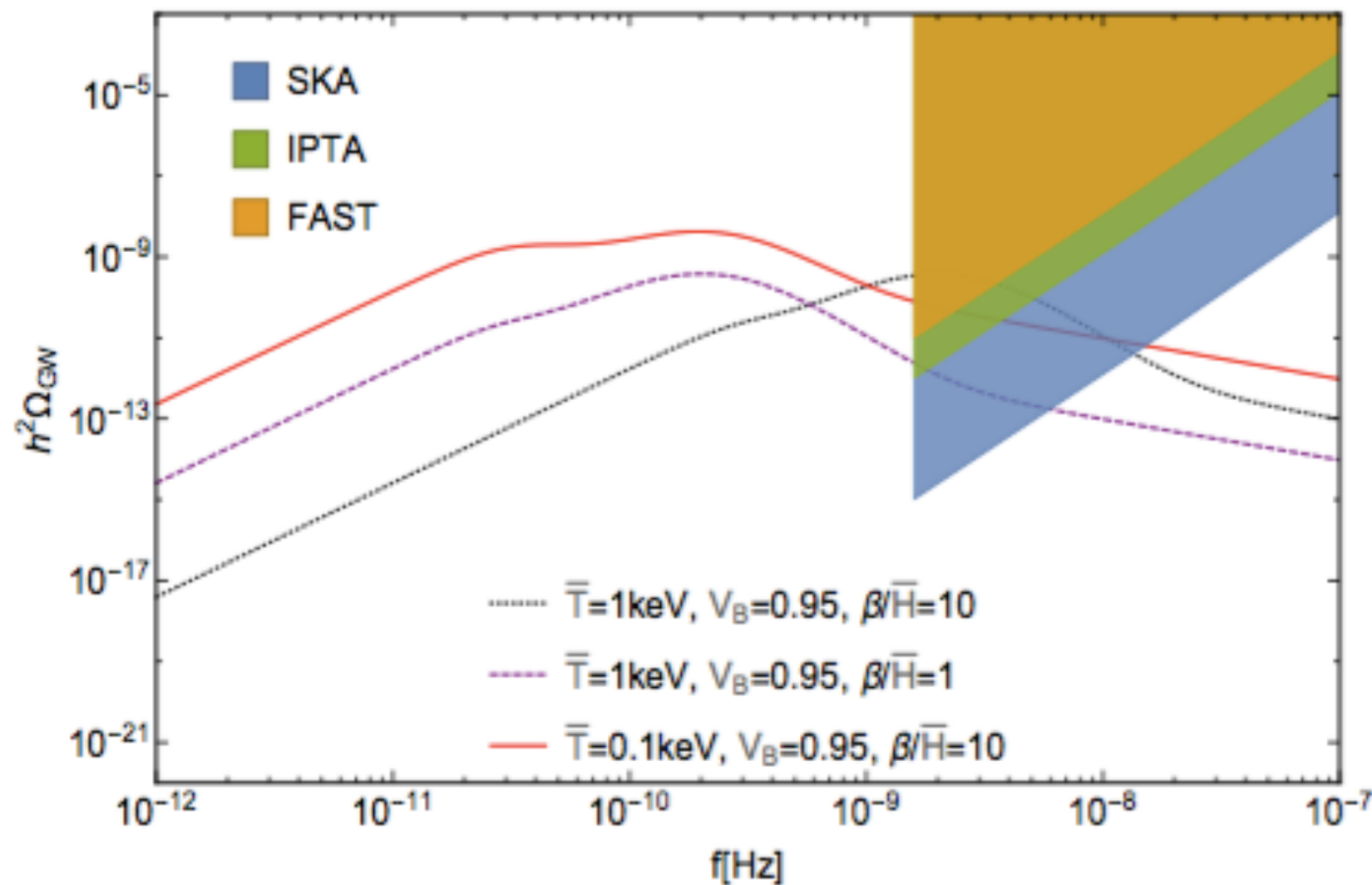A. Addazi & A. Marciano, CPC (2018), arXiv:1705.08346

FIG. 2. We report the limits from LHC and future CEPC (in brown and blu respectively), cosmological sphaleron bounds (green) and the region which will be probed by eLISA (red). The case of $\beta_2 = 1$ is displayed.

Constrained from radio telescopes at KeV scales

Type-I and Inverse See-saw with Majoron

For the majoron, $L(\sigma) = -2$ and mass terms read now:

$M\nu^c\nu^c \rightarrow Y_\sigma \sigma \nu^c \nu^c$ (type-I variant) $\mu SS \rightarrow Y_\sigma \sigma SS$ (low-scale inverse variant)

$\langle \sigma \rangle = \dfrac{v_\sigma}{\sqrt{2}}$ breaks spontaneously $U(1)_L \rightarrow \mathbb{Z}_2$

$M \rightarrow Y_\sigma v_\sigma / \sqrt{2}$ (type-I variant) $\mu \rightarrow Y_\sigma v_\sigma / \sqrt{2}$ (low-scale inverse variant)

Extended scalar sector:

$$V_0 = V_{\mathrm{SM}} + \mu_\sigma^2 \sigma^* \sigma + \lambda_\sigma (\sigma^* \sigma)^2 + \lambda_{h\sigma} H^\dagger H \sigma^* \sigma + \left(\tfrac{1}{2} \mu_b^2 \sigma^2 + \text{c.c.} \right)$$

Tiny $U(1)_L$ soft breaking term $\mu_b \sim \mathcal{O}(1\text{KeV})$

Resulting pseudo-Goldstone boson as testable DM candidate (Valle et '93, '07)

See-saw mechanism and GW production

See-saw gravitational footprint

High scale type-I seesaw with explicit U(1)$_L$ violation

$$\mathcal{L}_{\text{Yuk}}^{\text{Type}-\text{I}} = Y_\nu \bar{L} H \nu^c + M \nu^c \nu^c + h.c.$$

Heavy isosinglet neutrinos decouple from EW-scale: no FOPT and thus no GW signal from EWPT!

Low-scale inverse seesaw with explicit U(1)$_L$ violation

$$\mathcal{L}_{\text{Yuk}}^{\text{Inverse}} = Y_\nu \bar{L} H \nu^c + M \nu^c S + \mu S S + \text{h.c.}$$

Singlets closer to EW scale and sizable Higgs coupling

Thermal corrections from heavy neutrinos are not enough to induce FOPT

Fermions affect the potential at loop level, but still no FOPT !

Gravitational footprint of Lepton number SSB

Spontaneous breaking of U(1)$_L$ $\rightarrow$ Z$_2$ and inverse see-saw mechanism

Type-I variant
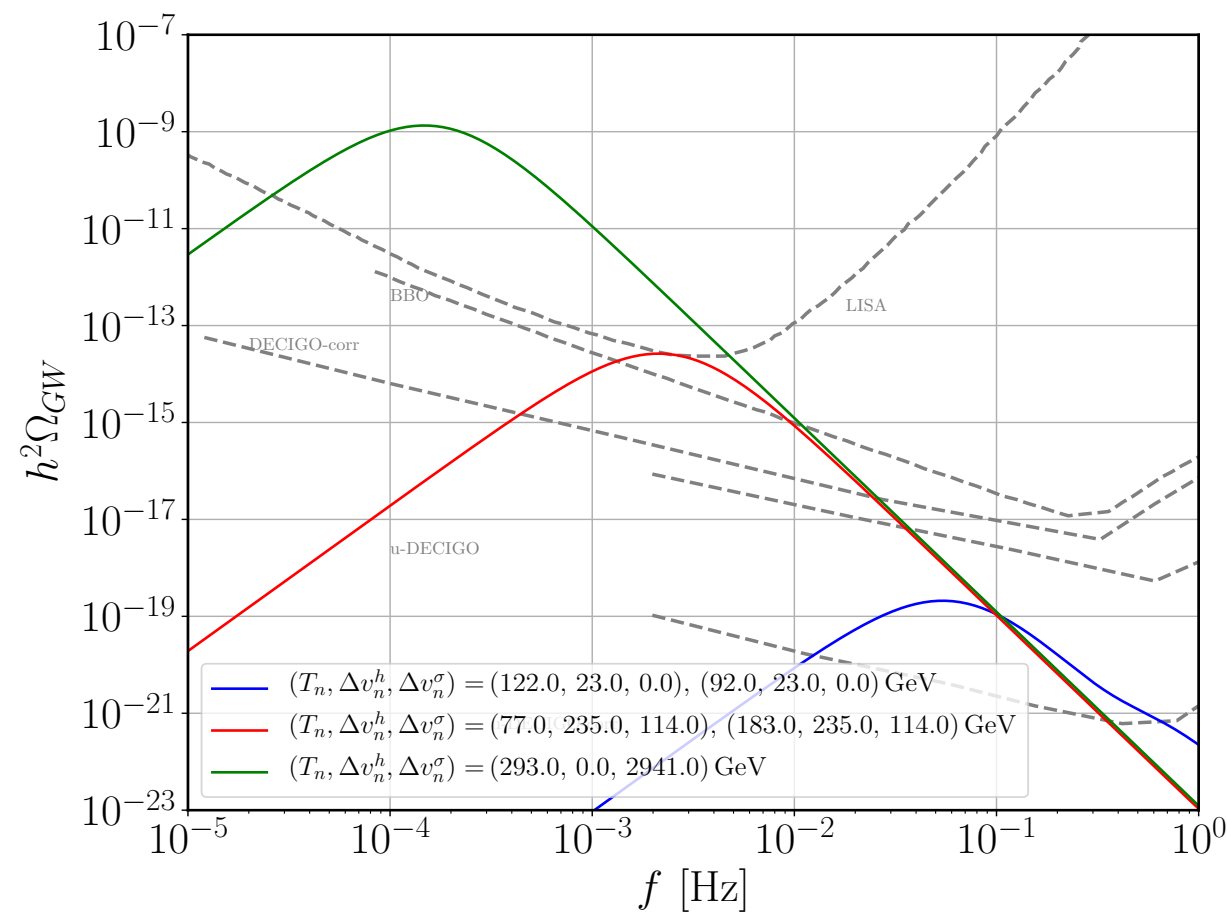
$$M\nu^c\nu^c \rightarrow Y_\sigma \sigma \nu^c \nu^c$$

Low-scale inverse variant

$$\mu SS \rightarrow Y_\sigma \sigma SS$$

Majoron scalar σ responsible for a new richer pattern of FOPTs

Inverse See-Saw with Majoron

Strength of PT enhanced by tree-level contributions

Characteristic signal with multi-peak scenario!

XXIII Bled (Virtual) Workshop, VIA platform, 6-10 July 2020

Richer patterns of FOPTs

Not only heavy isosinglet fermions couple to the Higgs → the Majoron complex scalar that breaks spontaneously U(1)$_L$ can couple substantially to the Higgs (modulo LHC)

$\downarrow$

Generation of two or three GW peaks

At the end of any FOPT scalar potential minimization requires non vanishing VEVs to be associated with the generation of EW and neutrino mass scales

Class I) $(0,0) \rightarrow (v_H, v_\sigma)$

Class II)
$$(0,0) \rightarrow (v_H, 0) \rightarrow (v_H, v_\sigma) \quad \text{for} \quad v_\sigma < v_H$$
$$(0,0) \rightarrow (0, v_\sigma) \rightarrow (v_H, v_\sigma) \quad \text{for} \quad v_\sigma > v_H$$

Class III)
$$(0,0) \rightarrow (v_H, 0) \rightarrow (0, v_\sigma) \rightarrow (v_H, v_\sigma) \quad \text{for} \quad v_\sigma < v_H$$
$$(0,0) \rightarrow (0, v_\sigma) \rightarrow (v_H, 0) \rightarrow (v_H, v_\sigma) \quad \text{for} \quad v_\sigma > v_H$$
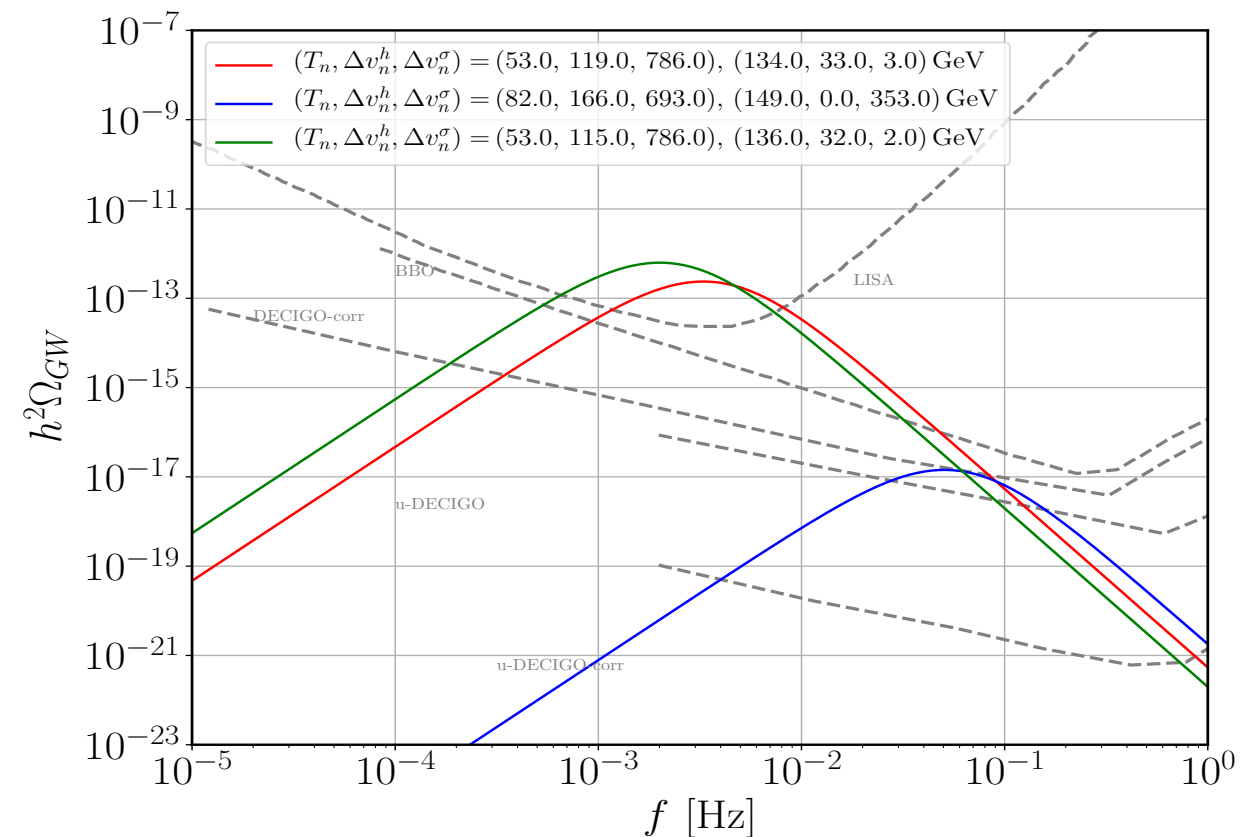
Three possible scenarios

Three possible scenarios, with nearly preserved U(1)L, namely $v\sigma\ (T = 0) \sim O\ (1\ keV)$

Peak Id	T_n	$(v_h^i, v_\sigma^i) \rightarrow (v_h^f, v_\sigma^f)$	α	β/H
Green 1	293	$(0,0) \rightarrow (0, 2941)$	0.5	4.9
Red 1	183	$(0, 114) \rightarrow (235, 0)$	7.7×10^{-4}	7.2×10^4
Red 2	77	$(0, 114) \rightarrow (235, 0)$	0.1	231
Blue 1	122	$(193, 0) \rightarrow (216, 0)$	1.4×10^{-2}	3.1×10^3
Blue 2	92	$(193, 0) \rightarrow (216, 0)$	9.4×10^{-3}	3.0×10^4

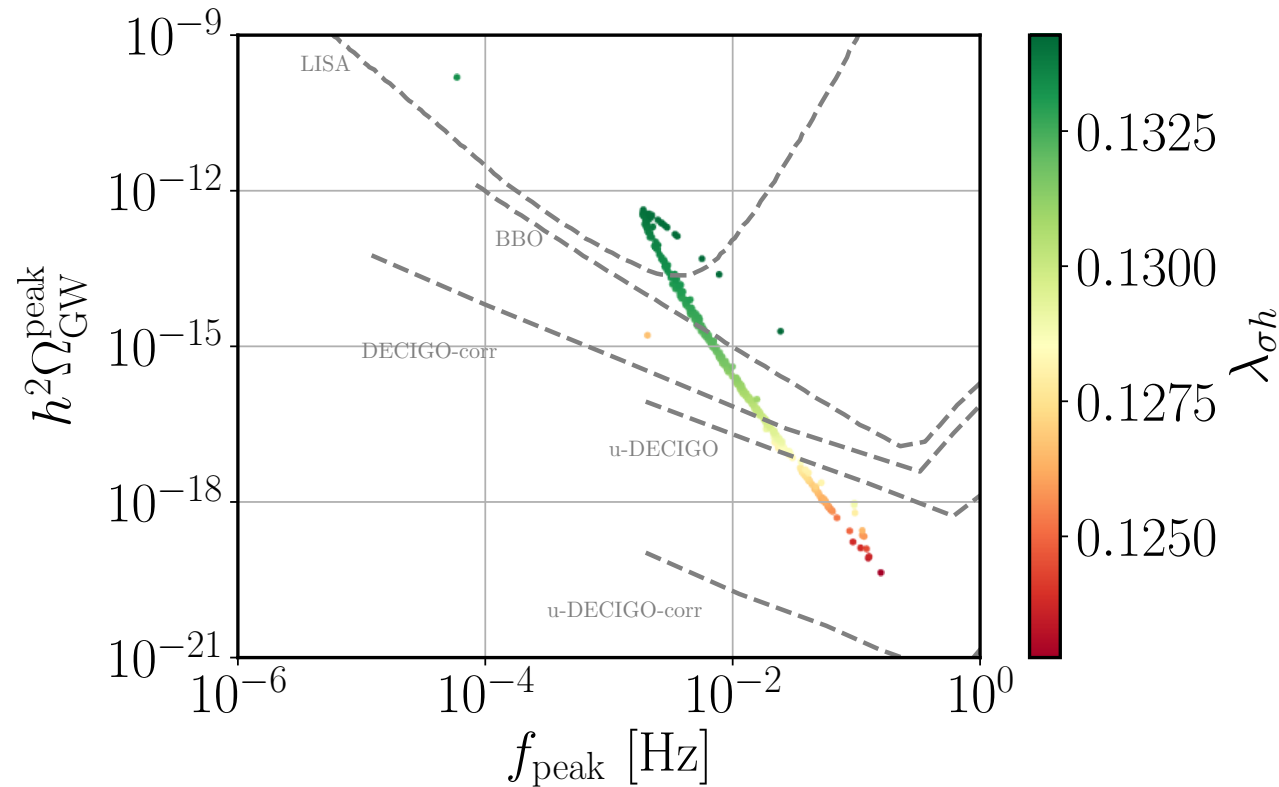| Curve	m_{h_2}	m_A	$\lambda_{\sigma h}$	λ_σ	M	Y_σ
Green	236	708	1.7	5×10^{-3}	380	2
Red	192	970	2.3	1.5	93	0.1
Blue	325	169	4	2.7	158	0.1

Detectable by **LISA**: very strong FOPT with $vn/Tn = 119$

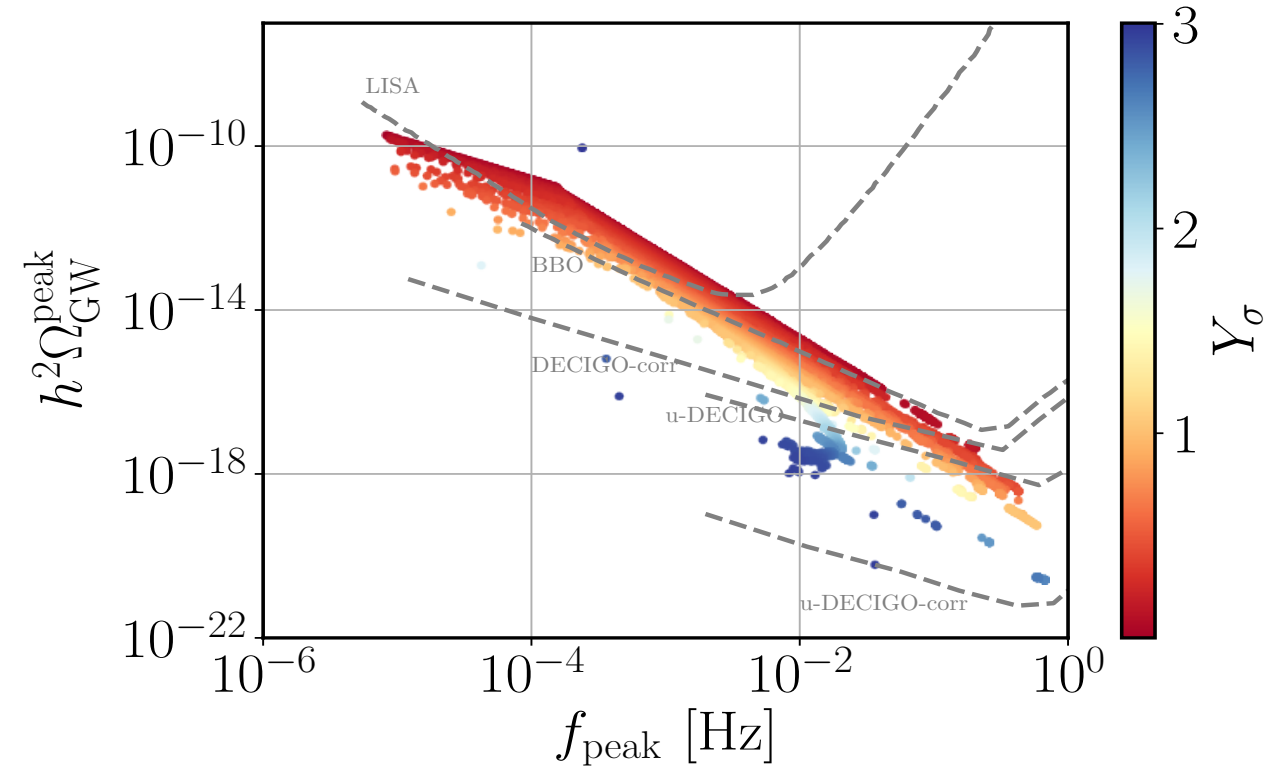(Consistent with invisible Higgs decays LHC bounds [Bonilla, Romão, Valle (2016)])

Two-peak scenarios detectable by DECIGO

Large quartic couplings enhance m/T and facilitate these scenarios: Bosonic $(m/T)^3$ contributions in $\Delta V^{(1)}$ (T) produce potential barriers

XXIII Bled (Virtual) Workshop, VIA platform, 6-10 July 2020

Multi-peak scenarios and generic features
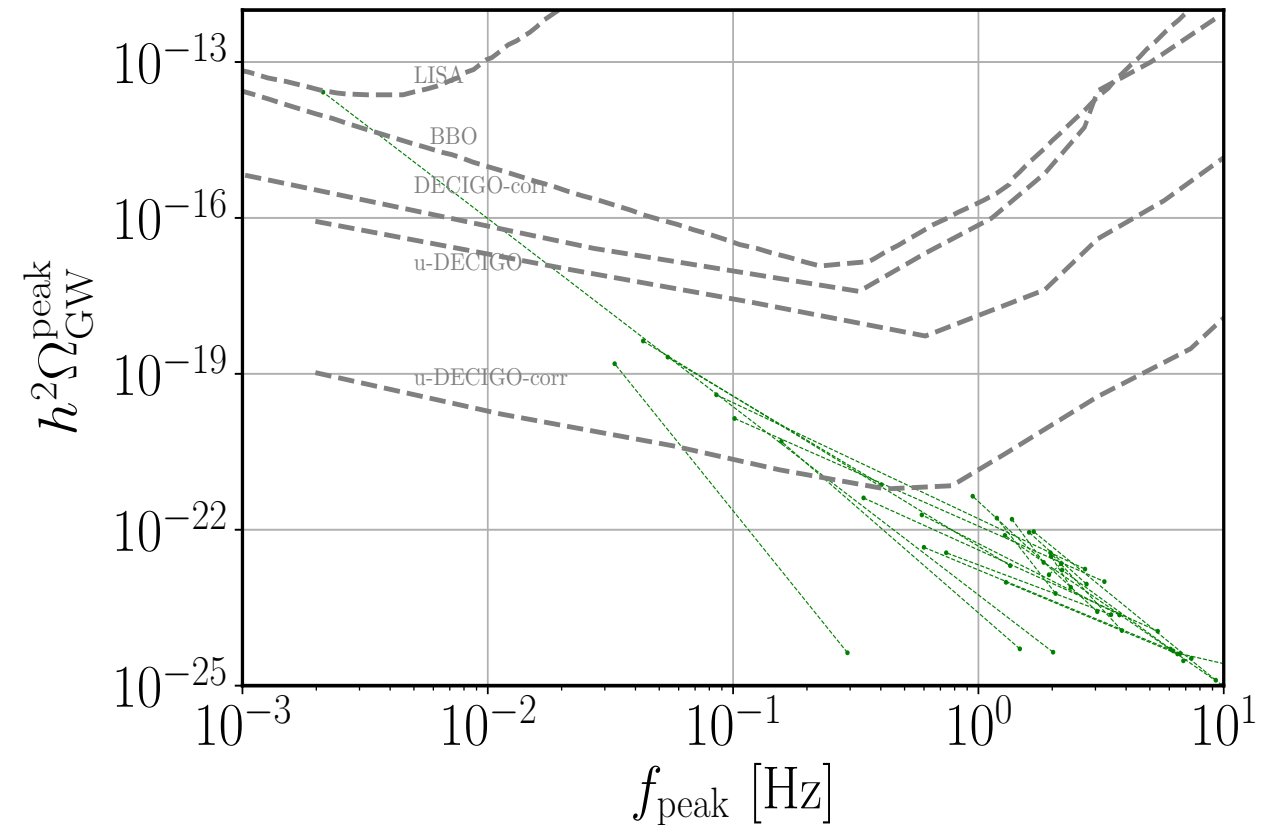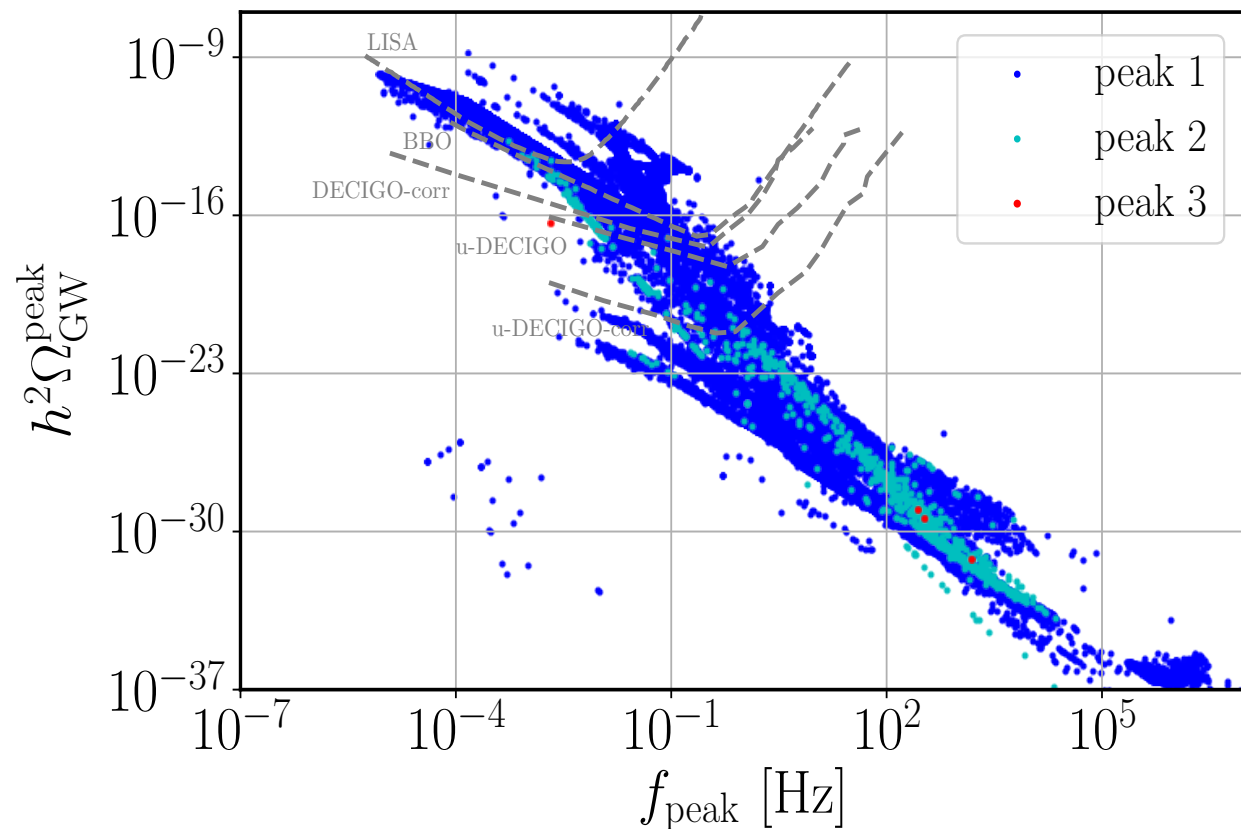

GW spectrum in λσh, for spontaneously broken
U(1)L .No solutions consistent with the LHC
bound on invisibly decays of Higgs

GW spectrum a in Yukawa coupling Yσ,
for softly-broken U(1)L (i.e. vσ = 0).
Order one variation of Yσ several order
of magnitude variations in the GW spectrum.

An order one variation in the Yukawa coupling reflects into violent variations by several orders of magnitude in
the GWs spectrum!

XXIII Bled (Virtual) Workshop, VIA platform, 6-10 July 2020

Multi-peak feature as a prediction of the Inverse seesaw with Majoron

Very hard to resolve the third peak

Multi-peaks only due to distinct phase transitions (no competition effect from the three mechanism, i.e. collision, sound waves, turbulence)

Possibility to distinguish/falsify neutrino mass generation mechanism

XXIII Bled (Virtual) Workshop, VIA platform, 6-10 July 2020
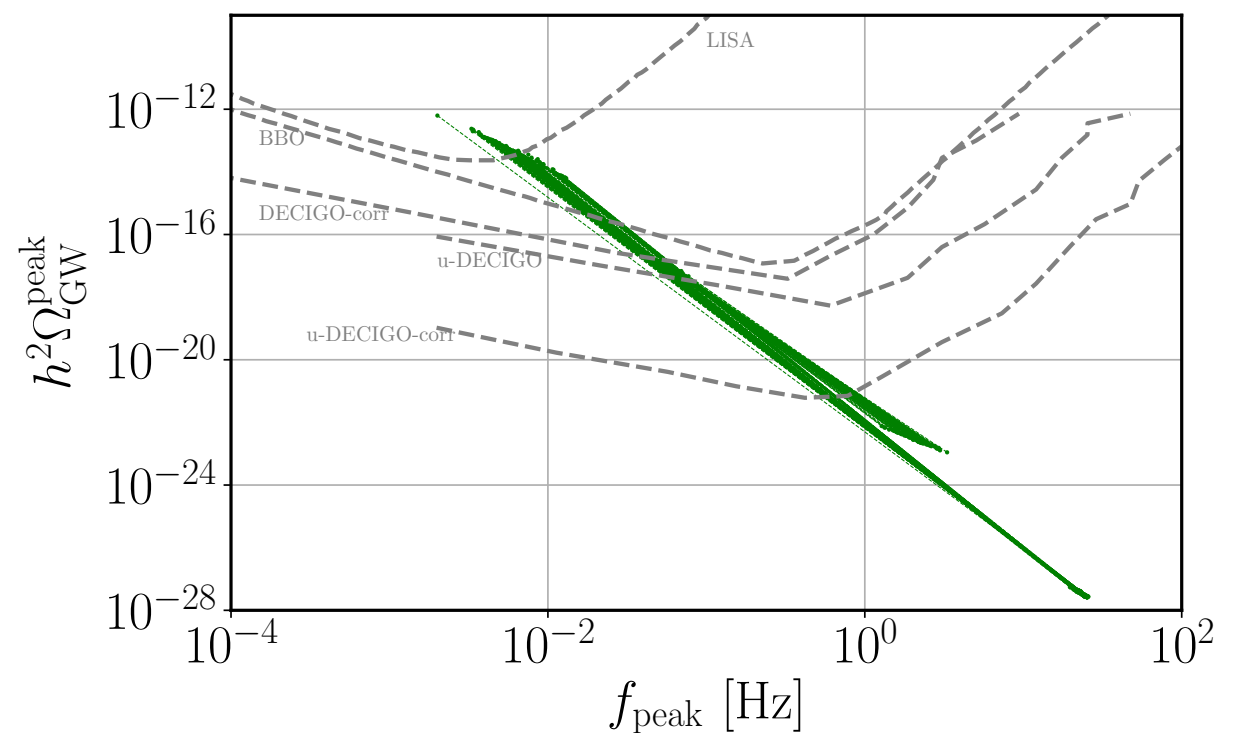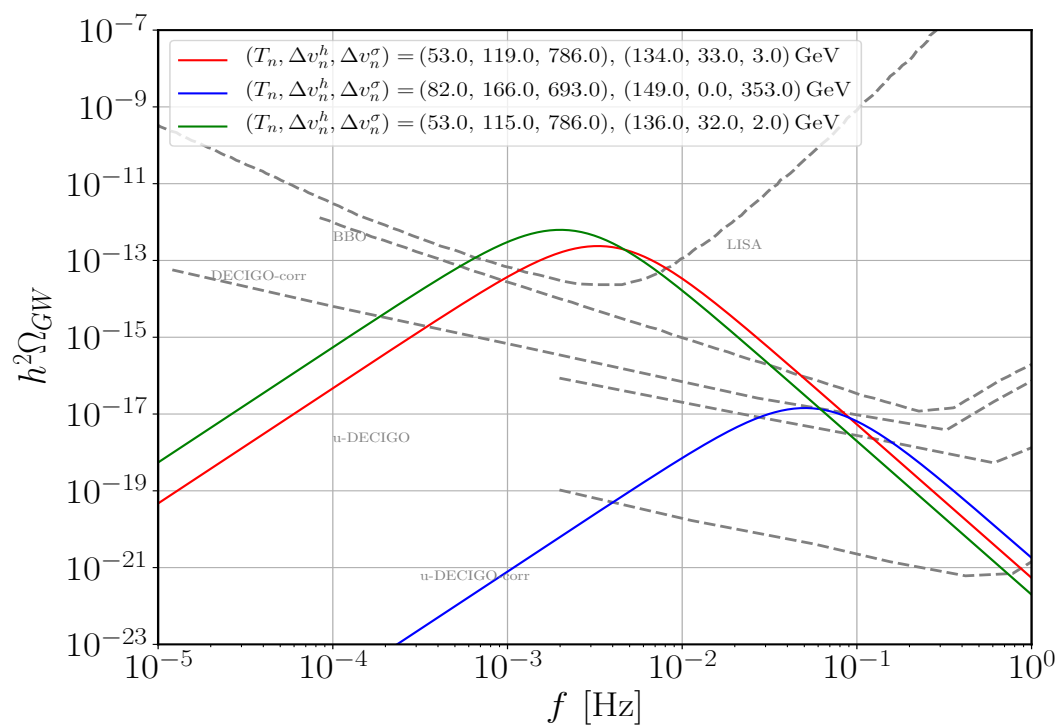
Type-I seesaw with Majoron

High scale variant: $Y_\nu \sim \mathcal{O}(1) \rightarrow M = Y_\sigma \nu_\sigma / \sqrt{2} \sim \mathcal{O}(10^{14} \text{GeV})$

for $Y_\sigma \sim \mathcal{O}(1)$ then $\nu_\sigma \sim \mathcal{O}(10^{14} \text{GeV}) \rightarrow$ NO FOPT

Low scale variant: $Y_\nu \sim \mathcal{O}(10^{-6}) \rightarrow M = Y_\sigma \nu_\sigma / \sqrt{2} \sim \mathcal{O}(100 \text{GeV})$

new states do not decouple: FOPT and GW are found

Less double peaks than in the Inverse See-Saw case, and mainly out of reach

XXIII Bled (Virtual) Workshop, VIA platform, 6-10 July 2020

Double-peak within experimental reach much rarer

In contrast to inverse seesaw + majoron one, PT is typically much stronger hiding the smaller peak

Curve	m_{h_2}	m_A	λ_h	$\lambda_{\sigma h}$	λ_σ	θ	v_σ	$Y_{\sigma,1}$	$Y_{\sigma,2}$
Green	203	188	0.14	0.03	0.03	0.26	790	0.07	1.58
Red	206	188	0.14	0.03	0.03	0.26	790	0.08	1.59
Blue	205	188	0.14	-0.02	0.03	-0.18	790	0.08	1.59

Peak Id	T_n	$\left(v_h^i, v_\sigma^i\right) \rightarrow \left(v_h^f, v_\sigma^f\right)$	α	β/H
Green 1	136	$(0, 921) \rightarrow (32, 919)$	9.4×10^{-5}	1.2×10^6
Green 2	53	$(245, 786) \rightarrow (360, 0)$	0.5	378
Red 1	134	$(0, 922) \rightarrow (33, 919)$	10^{-4}	1.1×10^6
Red 2	53	$(245, 786) \rightarrow (364, 0)$	0.5	612
Blue 1	149	$(0, 353) \rightarrow (0, 0)$	1.5×10^{-3}	1.0×10^5
Blue 2	82	$(205, 693) \rightarrow (40, 0)$	0.03	4.9×10^3

Second CP-even Higgs; $h = \cos\theta \, h_1 + \sin\theta \, h_2$

Consistency with Higgs invisible decays bounds assured

Conclusions

GW & tidal deformability as a probe of DM models and EoS of binary systems

Explicit lepton number violation cannot induce strong FOPT thus testable GW signals

Spontaneous U(1)L breaking leads to clearer GW footprints

Type-I seesaw and inverse seesaw (Majoron) models predict GW in the 0.1 -100 mHz

Different seesaw variants lead to distinct GW spectra!

Gravitational wave to shed light on the mystery of DM & neutrino mass generation!

Many caveats and issues to be solved: FOPT does not provide precisions physics!

谢谢

Спасибо

Thank you!

Grazie!

Static equilibrium and TOV

$$T^\alpha_\beta = Diag(\varepsilon, p, p, p) \qquad ds^2 = -e^{2\Phi}dt^2 + e^{2\Lambda}dr^2 + r^2 d\theta^2 + r^2(\sin\theta)^2 d\phi^2$$

$$G_{\alpha\beta} = 8\pi T_{\alpha\beta}$$

$$\nabla_\alpha T^{\alpha\beta} = 0$$

$$
\begin{cases}
e^{-2\Lambda} = 1 - \dfrac{2m(r)}{r} \\[2mm]
\dfrac{d\Phi}{dr} = \dfrac{1}{r}e^{2\Lambda}\left[8\pi^2 p(r) + \dfrac{2m(r)}{r}\right] \\[2mm]
\dfrac{dp}{dr} = -\left(p(r) + \varepsilon(r)\right)\dfrac{d\phi}{dr}
\end{cases}
$$

System is closed by an EoS: $p = p(\varepsilon)$